DESIGN OF A SUB-OPTIMAL DIGITAL CONTROLLER FOR AN ANTENNA CONTROL SYSTEM

by

J. H. Findeis

Submitted to the Department of Electrical Engineering

in partial fulfilment of the requirements for the degree

of

Master of Science

Department of Electrical Engineering

Faculty of Pure and Applied Science

University of Ottawa

Ottawa, Ontario

May, 1969

Approved for the Department
of Electrical Engineering

Supervisor

Chairman of the Examination
Committee

Chairman of the Department

ABSTRACT

This thesis deals with the design of a digital controller for a relatively complicated antenna system which contains several nonlinearities and is of a degree of complexity which makes a mathematical analysis of the control problem extremely difficult if not impossible.

The problem was approached by first simulating the system on a hybrid computer. Then, before the implementation of the experimental controller, attempts were made to obtain a representative mathematical model which could be used as a yard stick to measure the digital controller performance against a theoretical optimum.

A simplified model which gave satisfactory outputs for a variety of step inputs was obtained. The state equations were derived from this model and used in attempts to determine the theoretical optimum control for a step input command to the system. Two methods were used but both failed to yield useful results. Thus, instead of employing the theoretical solution as a standard of performance, a graphical approach was taken.

It was found that the control system was velocity limited for large step inputs. The graph of the position error of the system with a bang-bang controller thus represented an easily understood and relatively precise measure of the degree by which other control schemes fell short of achieving a true optimal control.

The type of control algorithm which was developed is easy to implement and has an almost minimum time response with no overshoot for step input commands. Antenna velocity is normally zero at both endpoints. In addition the algorithm makes possible the elimination of the compensation network. This is presently used to condition the command signals which are passed from the computer to the control system.

ACKNOWLEDGEMENTS

I would like to especially thank Dr. R. Gagne for his guidance and helpful suggestions in the development of the digital controller. My thanks also to Dr. L. Birta, Dr. I. Mufti and Mr. P. Trushel of the National Research Council for their comments and efforts in the attempted development of a theoretical optimal solution.

In addition I wish to express my sincere thanks to Professor J. Kruus for his valuable criticisms of this thesis and his beneficial supervision.

TABLE OF CONTENTS

Table of Contents -- Continued --

SYSTEM DESCRIPTION

1.1: Introduction

Canada's largest satellite communications ground station is located at Mill Village, N.S. It represents this country's contribution to the international global satellite communications system. The station has been in operation since late 1967. It is designed to handle traffic from two kinds of satellites; synchronous and non-synchronous ones.

Synchronous satellites have a period of rotation equal to that of the earth's, so that they appear stationary to the observer on the ground. They must, however, be located in the equatorial plane about 22,000 miles above the ground. The ground station in this case must track a barely moving object and position the antenna very accurately to assure lock-on. Because of the large distance between the station and the satellite a high gain communications channel is required. A high gain channel in turn implies a very narrow antenna beam and hence the need for the high pointing accuracy.

Non-synchronous satellites are not confined to the earth's equatorial plane and orbit at lower altitudes. When viewed from the ground station these satellites appear to sweep across the sky. The tracking system for such satellites must be able to move the antenna through a large range of angles and velocities. In this instance a relatively wide antenna beam would be advantageous to reduce the requirement of very precise positioning of the antenna before lock-on through the communications receiver can occur.

1.2: The Present Operational System

Due to the different tracking requirements for these two types of satellite systems, the antenna control system has to meet the conflicting demands of great pointing accuracy required by the high gain and narrow bandwidth of the communications receiver as well as good dynamic tracking to keep up with the large variations in velocity of the high speed, low altitude satellites. The control method therefore is a compromise between the extreme pointing accuracy required by the high gain loop and the ability to keep track of a relatively fast moving object for which a low gain loop is needed to permit quick responses to large angular changes.

The present acquisition and tracking system is required to operate in the following four modes:

1) Autotrack mode - the antenna tracks the satellite by means of analogue feedback. The autotrack receiver generates the pointing error signals which are used to correct the antenna position. For this mode to operate successfully the antenna must be pointing to within 0.1 degree of the satellite before a satisfactory lock-on can occur.
2) Manual mode - the antenna position is controlled by the operator through the motion of a joystick which drives a position synchro which in turn provides the error signal to the antenna.

3) Steering Tape mode - for low altitude, orbiting satellites there is the provision for receiving their orbital data and feeding this into the computer, which then can prepare a steering tape consisting of the time and desired position in increments of 5 seconds for the entire satellite pass. Shortly before the appearance of the satellite on the horizon, the steering tape is fed into the computer, which then determines the actual antenna position from digital shaft encoders on the antenna base and develops an error signal to feed to the control system taking into account the actual time and the desired antenna position.

4) Designated Position mode - the desired position of the antenna is determined by a number stored in the computer memory. The actual antenna position is fed into the computer via the digital shaft encoders and the computer calculates the appropriate error voltage [1].

The latter mode is the one for which the digital controller has been designed. The elevation axis alone has been considered because it is less complex. The cross-coupling effect between the elevation and azimuth axis were assumed to be negligible, so that a successful control scheme for one axis should prove to be equally useful for the other one.

Under present operating conditions for step input commands the antenna oscillates about the desired position before coming to rest. One of the

causes of this imprecise control is the digital-to-analogue (D/A) converter. It transforms the control signal into a voltage level, but limits for angular error outputs of 0.5 degrees or more. This voltage level remains at the maximum value until the error between the actual antenna position and the desired one is less than 0.5 degrees. Then the error signal decreases linearly until it becomes zero when the antenna position error is zero. If we assume that the antenna is being driven toward its desired position and has reached its maximum velocity, then the control signal to supply a reverse torque and thus stop the antenna motion will not be issued until the positional error is actually equal to zero. The momentum of the antenna at this point is still so large that it overshoots its desired position enough to cause the D/A converter to limit in the opposite direction. This oscillatory process results in an underdamped system response.

The achievement of good dynamic performance of the antenna system is made more difficult by the physical size of the various parts. The antenna, for instance, consists of an 85 foot parabolic dish weighing 240 tons. In the elevation axis a 5 HP electric motor supplies the necessary motive power for positioning the antenna dish through a 12,000:1 gear ratio. In order to simplify this control task, the entire structure is enclosed in an inflatable radome.

To improve the system response without incurring large additional hardware costs, a digital controller scheme was proposed which would result in a more highly damped system, so that the antenna would reach its final position in minimum time with little or no overshoot. It was also deemed desirable to increase the system reliability by reducing

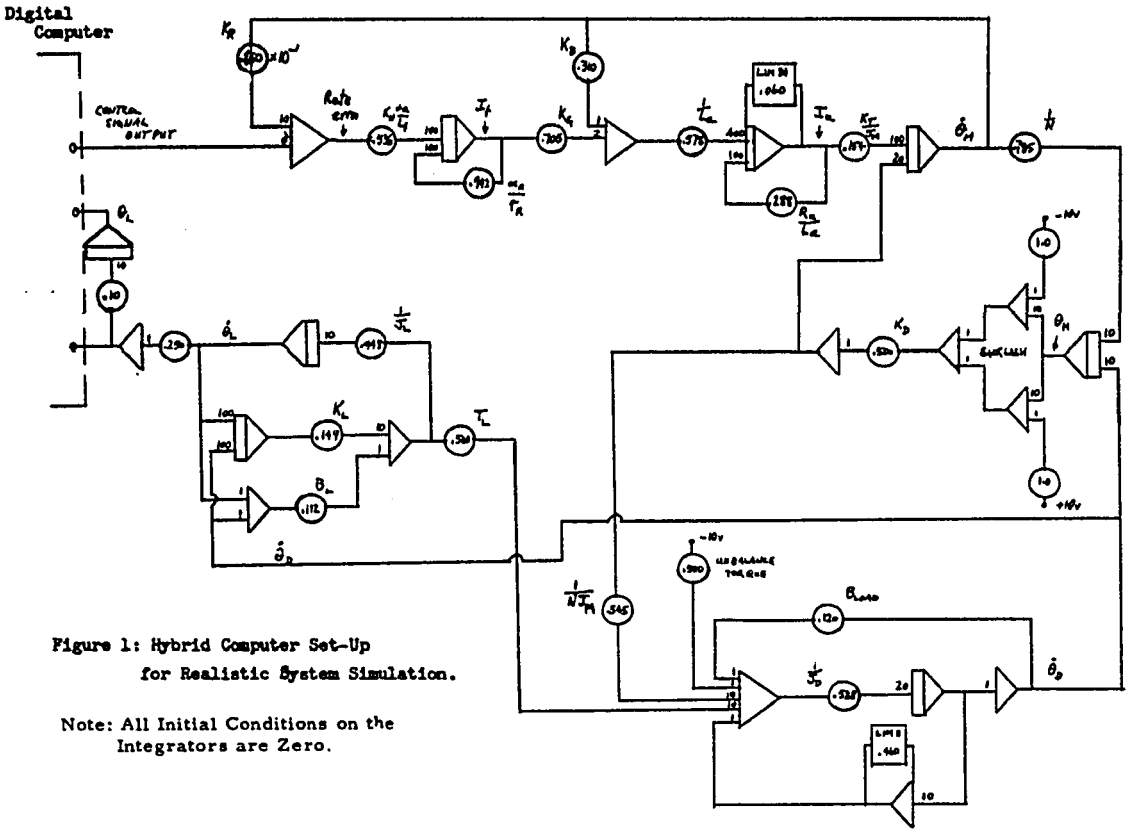

Figure 1: Hybrid Computer Set-Up for Realistic System Simulation.

Note: All Initial Conditions on the Integrators are Zero.

B_L	Structural Damping	Lb-Ft/(Rad/Sec)
B_{Load}	Load Damping at Gimbal	Lb-Ft/(Rad/Sec)
I_a	Armature Circuit Current	Amps
I_f	Generator Field Current	Amps
J_D	Structural Inertia	Lb-Ft/(Rad/Sec)
J_L	Structural Inertia	Lb-Ft/(Rad/Sec)
J_M	Motor Inertia	Lb-Ft/(Rad/Sec)
K_B	Motor Back-EMF Constant	Volts/(Rad/Sec)
K_D	Structure Spring Constant	Lb-Ft/Rad
K_G	Generator Constant	Volts/Amp
K_L	Structure Spring Constant	Lb-Ft/Rad
K_N	Rate Loop Amplifier Gain	Volts/Volt
K_R	Rate Feedback Gain	Volts/(Rad/Sec)
K_T	Motor Torque Constant	Lb-Ft/Amp
L_a	Armature Circuit Inductance	Henries
L_f	Generator Field Inductance	Henries
N	Gear Ratio	--
R_a	Armature Circuit Resistance	Ohms
T_L	Structural Torque	Lb-Ft
τ_R, $\frac{1}{\tau_R}$	Rate Loop Lead-Lag Compensation	
θ_D	Gimbal Rotation	Radians
θ_L	Structure Rotation	Radians
θ_M	Motor Rotation	Radians

the number of components in the control loop. By increasing the computational load on the digital computer, the analogue compensation network can be eliminated. The main reason for the design of the digital controller was, however, the desire to achieve a minimum or near minimum time transfer of the antenna between any two positions with zero velocity and acceleration at both end points.

1.3: The Analogue Model

Initially the analogue portion of the system was simulated by the Dalmo Victor Company of Belmont, California [2]. The model from this simulation study was duplicated by J.A. Dolan and the author, on the PACE analogue computer at the Analysis Section, Division of Mechanical Engineering, National Research Council, Ottawa. The simulation then was made more realistic by replacing the analogue summer in the control loop with a digital computer. Additional saturation limits which correspond to physical limits in the actual control system were also included. The result of this endeavour proved that the dynamic and steady state characteristics of the analogue computer model were close to those of the actual system. The findings are documented in [3].

The diagram of the hybrid computer set-up is shown in Figure 1. For the development of the digital controller, the model was simulated on the EAI hybrid computing facility of the Mechanical Engineering Division of the National Research Council. Most of the physical system components were simulated on the analogue computer, while the determination of the appropriate control signal was carried out by the digital computer as a result of the stored algorithm.

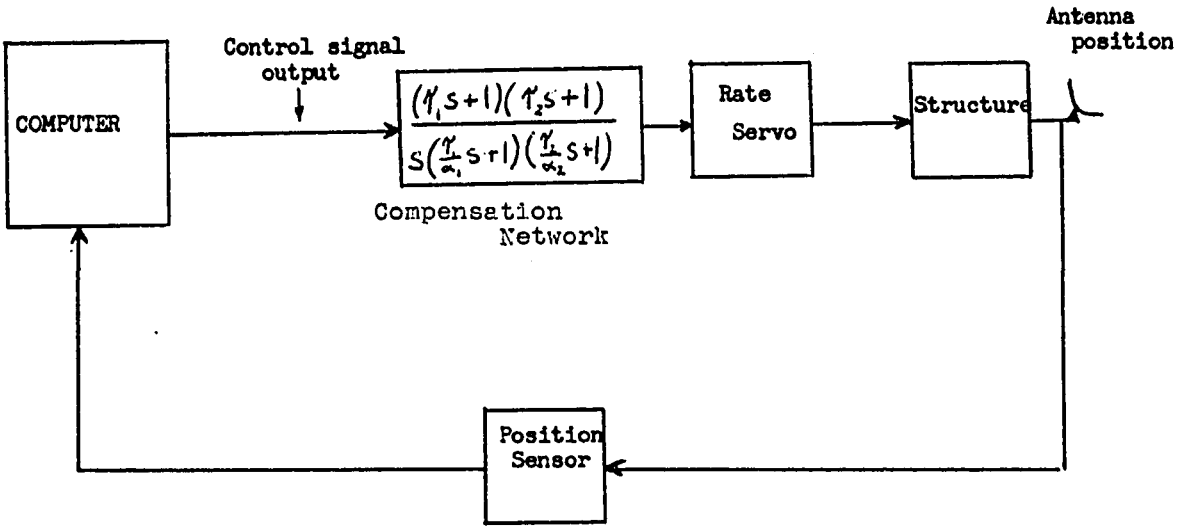

Figure 2: Present System in the Designated Position Mode.

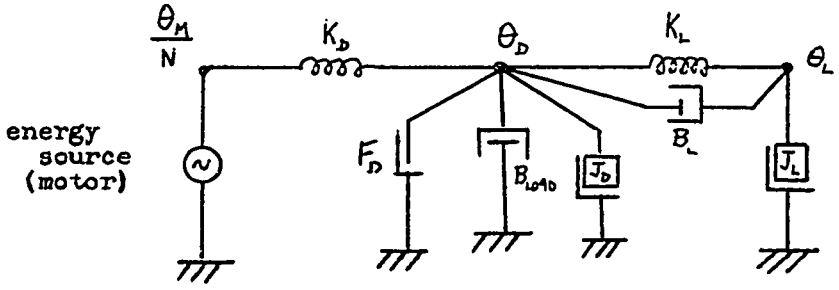

where
N - gear ratio
K_D - drive spring constant
B_{LOAD} - load damping at gimbal
B_L - structural damping
K_L - load spring constant
J_D - drive inertia
J_L - load inertia
θ - angular displacement
F_D - drive friction

Figure 3: Physical Model of Antenna and Drive Train.

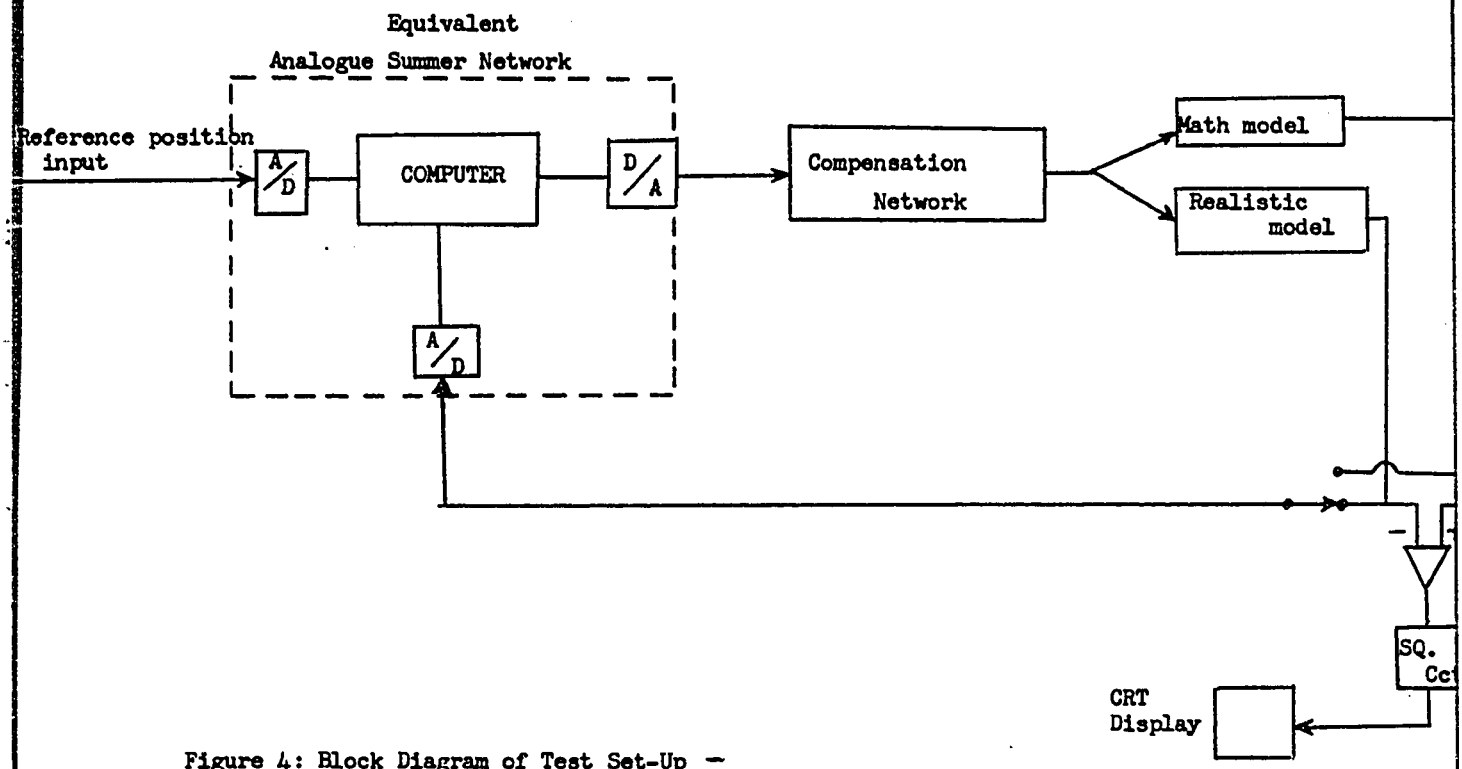

Figure 4: Block Diagram of Test Set-Up –
Determination of Mathematical Model Transfer Function.

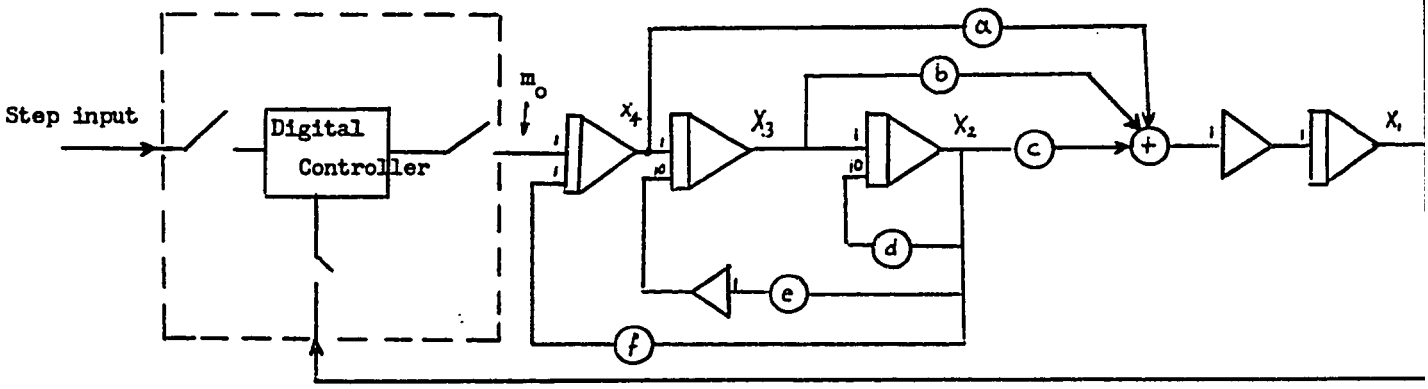

Figure 5: Analogue circuit representation of $\frac{as^2+(b+ad)s+c}{s(s^3+ds^2+es+f)}$

1.4: The Basic Antenna Control System

Figure 2 shows in block diagram form the present system for operation in the Designated Position Mode. The mathematical representation of the compensation network is also given. This network conditions the output control signal from the computer. The rate servo block has as input this modified control signal. It is compared to the feedback voltage provided by a tachometer mounted on the motor output shaft. The resultant output then controls the field current of a generator which in turn drives the motor.

Figure 3 is an elaboration of the antenna structure block. It is the physical representation of the analogue computer model and is taken from [2]. Only the vertical axis control system is shown. The structural dynamics of the antenna and its drive are simulated by a two-mass, two spring model which takes into account the non-linear effects of friction and back-lash in the gear train. Due to the complexity of this model no attempt was made to determine theoretically the minimum time open-loop control sequence. Such a sequence would result in moving the antenna in as short a time as possible from rest in one position to another position also at rest.

THE MATHEMATICAL SYSTEM MODEL

One form of analytic solution that was attempted was the derivation of a simplified model which was analytically tractable and still had the same response for a specific class of inputs as the real system. The class of inputs used in this case was a series of step inputs of various amplitudes.

In order to be assured of a realistic minimum time solution for our problem, we attempted to derive a theoretical optimal control solution for a standard of comparison. We were therefore trying to solve a minimum time problem. This theoretical solution was of necessity based on the analysis of the simplified model which we shall refer to as the mathematical model in the future. This model had to contain at least one nonlinearity in order to obtain a good response agreement. One saturating type nonlinearity representing the output limits of the control signal D/A converter was therefore retained in the mathematical model.

The block diagram of the test set-up is shown in Figure 4. Various kinds of simple, linear transfer functions were constructed on the analogue patchboard and connected into the circuit as the mathematical model. A variety of step inputs ranging from 0.5 to 20 degrees were then applied to the system and all the transfer function parameters varied to see if a response similar to the real system response could be obtained for the entire range of step inputs. Initially the responses of the closed loop real antenna system and the mathematical model were displayed on an oscilloscope and the parameters were adjusted so that the visually displayed curves were as similar as possible. For finer adjustments, the

square of the error of the open-loop mathematical model and the closed loop antenna system was displayed. The performance criterion used to determine the best fitting model was that of minimizing the integral $\int_0^{T_2} e^2 dt$ where e is the realistic antenna system response minus the simplified model response for the entire range of step inputs from 1 degree to 20 degrees. T_2 is a fixed time interval of approximately 15 seconds.

The model which gave the best results was a limiter followed by a fourth order transfer function of the form $\frac{As^2+Bs+C}{s(s^3+Ds^2+Es+F)}$. The analogue circuit configuration of this transfer function is shown in Figure 5. The analysis of this simplified representation of the antenna control system was then attempted. Since the model's response to step inputs was similar to the step responses of the real system (see graphs #5 and #7) for the entire range of step inputs, it was hoped that any theoretically derived optimum control for the model would serve as a yardstick for measuring the effectiveness of experimentally obtained solutions for the original nonlinear case.

THE THEORETICAL OPTIMAL CONTROL SEQUENCE

3.1: Selection of Methods for the Development of the Optimal Control Sequence from the Mathematical Model

From the analogue patchboard configuration of the mathematical model we obtained the corresponding state variable representation and its A matrix. (See Appendix A). The coefficient matrix is defined by the general vector matrix equation [5]:

$$\frac{d\bar{x}(t)}{dt} = A\bar{x}(t) + D\bar{m}(t)$$

where $\bar{x}$ = state vector

$\bar{m}$ = control vector

A = coefficient matrix

D = driving matrix

We assume that the saturating nonlinearity is considered as an upper and lower bound on the control signal m. Another assumption is that the initial conditions are always zero. This is justifiable since the need for a control input to the antenna system only arises when the antenna position has to be changed. Thus the system will have ample time to return to rest between two successive new reference inputs.

Starting with the initial conditions of the system at rest, the state vector is $\bar{x}^T(0) = [0\ 0\ 0\ 0] = [x_1 x_2 x_3 x_4]$ where x_1 is the antenna position. (All the remaining state variables have no physical significance.) In this particular case at the completion of the control sequence, x_1 should equal the desired angle and all other state variables should once again equal zero. This formulation of the problem yields therefore a fixed end point problem with a bound on the control input. A general algorithm has been developed by L. Birta and P. Trushel

[4] of the National Research Council which calculates the open-loop optimal control sequence that transfers a system from an initial state to a final state in minimum time. The algorithm is designed to obtain the desired control sequence from the state variable representation. This was the first attempt to obtain a theoretical solution.

The second approach was to employ Tou's method [5] of iteratively premultiplying the state vector by the feedback matrix and the state transition matrix. Both these matrices were developed from the state variable representation as outlined in Appendices A and B. This method yielded a control sequence for the closed-loop system. Since the control signal sequence is generated inside the forward loop of the feedback system, both closed loop and open loop calculations should have yielded the same result at that point in the system and thus a comparison was possible.

The third method involved the empirical determination of the control sequence through the use of the hybrid computer model.

3.2: Development of the Closed-Loop Optimal Control System

Although the calculation of an optimal open loop sequence was theoretically feasible, it could not have been implemented in an actual operating system without incorporating some means of antenna position feedback to the controller. Only through some manner of feedback could the effects of system noise, parameter variations and other inaccuracies, which were neglected in the calculations of the control sequence, be overcome.

The best means of calculating the response of a closed loop system to a step input command appeared to be by means of the method outlined by Tou [5]. By using this method the value of the state variables is calculated

at every sample point. Since the control sequence is not one of the state variables, it cannot, therefore, be calculated directly.

To determine the optimal control sequence, consider the vector matrix differential equation

$$\dot{\bar{x}}(t) = A\bar{x}(t) + D\bar{m}(t) \qquad \text{(1-A)}$$

where m(t) is the input to the digital controller and

$$m(t) = m(nT^{+}) \text{ for } nT < t \leq (n+1)T$$

T in the above equation represents the sample interval. The solution to equation (1-A) can be written as:

$$\bar{x}(t) = e^{A(t-t_0)}\bar{x}(t_0) + \int_{t_0}^{t} e^{A(t-\tau)} D\bar{m}(\tau)\, d\tau \qquad \text{(1-B)}$$

Now if we define $\phi(t) = e^{At}$ as the transition matrix of the process, then (1-B) can be rewritten as:

$$\bar{x}(t) = \phi(t-t_0)\bar{x}(t_0) + \int_{t_0}^{t} \phi(t-\tau) D\bar{m}(\tau)\, d\tau \qquad \text{(1-C)}$$

For the interval $nT < t \leq (n+1)T$ equation (1-C) becomes

$$\bar{x}(t) = \phi(t-nT)\bar{x}(nT^{+}) + h(t-nT)\bar{m}(nT^{+}) \qquad \text{(1-D)}$$

where h(T) = control transition matrix

$$= \int_{0}^{T} \phi(T) D\, d\tau$$

If we let $t = (n+1)T$, then we can rewrite equation (1-D) as follows:

$$\bar{x}[(n+1)T] = \phi(T)\bar{x}(nT^{+}) + h(T)\bar{m}(nT^{+})$$

If the forcing function $\bar{m}(nT^{+}) = 0$, then the preceding transition equation becomes:

$$\bar{x}[(n+1)T] = \phi(T)\bar{x}(nT^{+})$$

From the above equations it becomes apparent that the state vectors of the plant for any two consecutive samples are related through the premultiplication by the transition matrix $\phi(T)$. Similarly we can relate the forcing function state vector for any two consecutive sampling instants by the equation:

$$\bar{m}[(n+1)T] = R(T)\,\bar{m}(nT^+)$$

Combining the input state vector $\bar{m}$ and the plant state vector $\bar{x}$ yields the total state vector: $\bar{v}(t) = \begin{bmatrix} \bar{m}(t) \\ \bar{x}(t) \end{bmatrix}$

Again $$\bar{v}[(n+1)T] = \Phi(T)\,\bar{v}(nT^+) \qquad (2)$$

where now $$\Phi(T) = \begin{bmatrix} R(T) & 0 \\ h(T) & \phi(T) \end{bmatrix}$$

For any given system, one can readily determine a matrix B, which describes the relationship existing between the state vector before and after sampling, for instance in our case

$$\bar{v}(nT^+) = B\,\bar{v}(nT) \qquad (3)$$

Since the effect of feedback in a sampled data system is felt only after each sampling instant, the B matrix will be referred to as the feedback matrix.

Now the above equations (2) and (3) can be used in an iterative manner to determine the values of the state variables at successive sample intervals. Since we are given the initial values of the state vector $\bar{v}$ and have determined both the transition matrix and the feedback matrix from the state variable representation we can obtain successive values of the state vector through straightforward mathematical manipulations.

One complication that this method includes is the calculation of the 'effective gain' of the digital controller which is in the control loop and therefore must be reflected in the state transition matrix. The controller, together with the saturating non-linearity, is considered as a variable gain element K_v, which can assume different values at successive sampling instants but is constant during each sampling period. The input to K_V is the signal m, the error signal, which is derived internally in the computer from the reference input and the actual antenna position. The output is termed m_o as shown in Figure 5.

In order to obtain the value of K_V for any particular sampling instant consider the n^{th} interval. For any sampling period the input and output of the variable gain element are related by a constant K_n

$$\text{where} \quad m_o(nT^+) = K_n m(nT^+) \tag{4}$$

and K_n is the gain constant during the n^{th} sampling period. We can rewrite equation (4) as $K_n = \frac{m_o(nT^+)}{m(nT^+)}$

As long as the resultant $K_n \leq 1.0$, the system is still in the saturating region and the output of the nonlinear element will remain at one of its bounds. The value obtained for K_n in the preceding equation is then substituted into the transition matrix $\phi_n(T)$ where the subscript n denotes the n^{th} sampling instant. Then by application of equation (2) the entire state vector at the (n+1)st sampling instant can be calculated. Once equation (4) yields a $K_n > 1.0$, then the nonlinearity is no longer affecting the system performance since the bound on the signal will no longer be reached. From then on we are dealing strictly with a fourth order, linear system which will require at the most four sampling instants to return to the origin or steady state conditions. This has been proven by Bellman [6].

The conditions for linearity are only satisfied, however, if no other nonlinearities start affecting the system's performance as the reverse torque is applied to bring the antenna to a halt. No attempt was made to develop a real time algorithm which would solve for the sampling intervals of the final four output commands. Such a task cannot be carried out in real time control situations without considerable difficulty if one is using a process computer with a small memory capacity. In addition, once the system enters the so-called unsaturated region, the control signal outputs are very time dependent, so that they would have to be initiated by external real time clock interrupts to determine the precise instant of sampling. This situation would require some program changes as no such clock interrupts are used in the algorithm. The program continues circulating through the logic chain, branching as required. The timing estimates to assure an adequate sampling frequency are based on the longest sequence of program steps.

In the calculation of the optimal output commands it is also not possible to make allowances for any variation of the operating system parameters and the inaccuracies of the fit of the mathematical model. Clearly for a working system centred around a small control computer with sampling periods of 30 milliseconds or less required for precise antenna control, a different approach to achieving optimal or near optimal control is desirable.

EXPERIMENTAL DIGITAL CONTROLLER DESIGN AND EVALUATION

4.1: Description of Algorithms Leading to the Final Control Scheme

The philosophy employed in designing the control algorithm was to keep the computational time of the central processor to a minimum in order to permit the computer to carry out other necessary functions. It should be noted that in the algorithm for the model, additional central processor time is used in excess of the needs of the operational algorithm. This time is used to investigate the effects of a change in the width of the proportional control region as well as variations in the amplitude of the saturating signal on the system response time. The width of the proportional control and the saturating signal amplitude will remain constant in the operating system and will not be sampled at regular intervals as they were in the test set up.

Initially several methods of improving the small error sensitivity of the algorithm were investigated. To date there have been no requirements for maintaining the antenna at any specified angular position in the Designated Position Mode for any length of time. Normally lock-on through the receiver system occurs as soon as the antenna is pointing to within the required 0.1 degrees and the antenna velocity is less than 0.15 degrees per second. The usefulness of the algorithm could, however, be extended to the Steering Tape Mode if a precise enough means of correcting very small pointing errors could be devised without causing instabilities in the system.

The first program (Algorithm-1) had one switching point between a region of maximum signal output and the proportional region as shown in

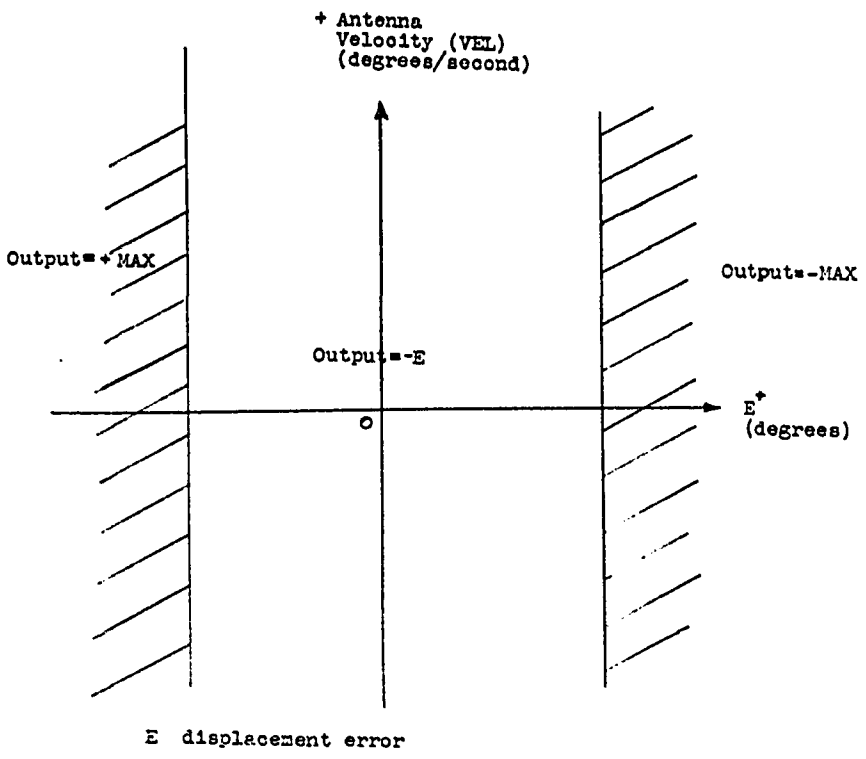

Figure 6: Switching Graph for Algorithm-1.

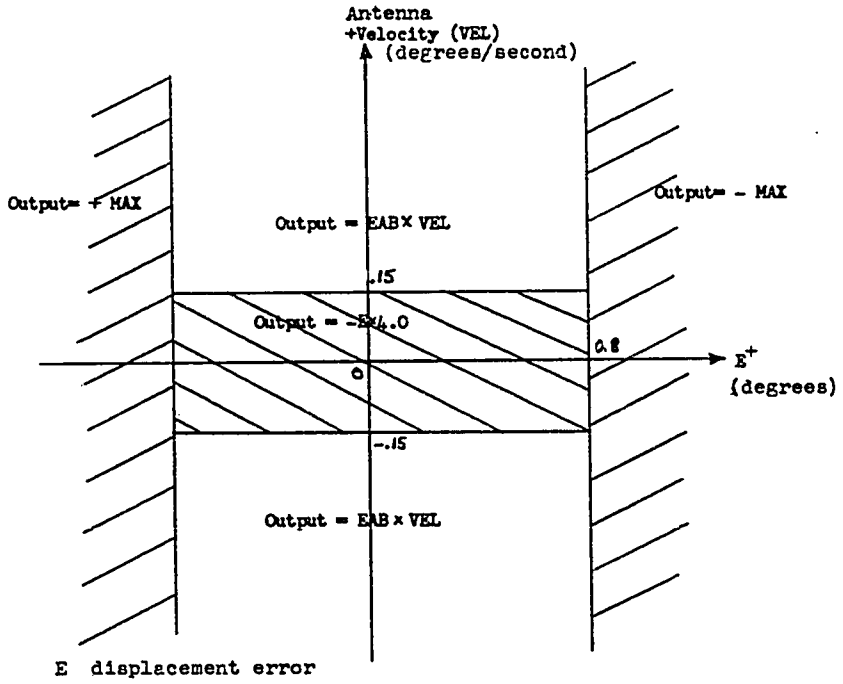

Figure 7: Switching Graph.

Figure 6. In the proportional region, when the control signal was made directly proportional to the displacement error, a large limit cycle resulted with an unstable response for some step inputs. This was due to the high system gain. By reducing the loop gain we achieved adequate control with this method, but it also meant a longer time interval to achieve a designated angular change. Then the proportional region was modified to result in a multiplicative type of control so that the error signal was the product of velocity and error displacement (Algorithm-2). This scheme suffered from the shortcoming that as the antenna approached its desired position, its velocity approached zero and the controller became insensitive to very small pointing errors. This lack of sensitivity was due to the fact that for slight angular errors and low antenna velocities two very small numbers are multiplied in the computer to yield the multiplicative control signal. The most significant sixteen bits of the product are thus equal to zero. Since the control signal amplitude is related directly to those sixteen bits, it is also equal to zero before the desired position is actually reached. To overcome this shortcoming a second switch point was introduced, so that the program changes from the multiplicative region of Algorithm-2 to a truly proportional region for velocities <0.15 degrees per second. This last change finally resulted in a program (Algorithm-3) which provided a satisfactory system performance.

The advantages of a multiplicative control scheme have been indicated by M. Jafri [7] and the apparent increase in the damping of the system appears to be at least partially a result of employing this type of control.

4.2: Description of Control Algorithm-3

The flow diagram shown as Appendix C outlines the final version of the digital controller program. The controller provides near optimal control, minimizing the integral $\int_0^{t_1} dt$ where t_1 represents the final time for the antenna to come within ± 0.1 degrees of the desired position. The normal step inputs which are expected to be handled by the controller have amplitudes in excess of 2 degrees. The control scheme is independent of the sampling frequency provided that it is kept at or above 33 samples a second. At slower rates the discontinuities of successive output commands start to affect the present system performance. This is one of the findings mentioned in [3]. Since the program is a closed loop algorithm it provides the normal benefit of feedback control to the system, so that the latter's step responses are similar for a considerable range of the system parameter values. The diagram shown in Figure 7 is a graphical means of showing the decision space which determines when the program switches from the maximum drive signal to a proportional or multiplicative mode as determined by the displacement error and the antenna velocity. In order to achieve satisfactory step responses, the sign and magnitude of the antenna velocity as well as the sign and magnitude of the error displacement had to be included in the control scheme. This presented no problem as far as the simulation was concerned, as error velocity was obtained from the output of an integrator the input of which represented antenna acceleration. In the operational system the output voltage of the tachometer mounted on the motor drive shaft represents antenna velocity, so that connecting an analogue to digital converter to the tachometer will suffice to provide the computer with the sign and magnitude of the antenna velocity.

As soon as the step input is provided, the computer samples the variables of desired antenna position, actual antenna position and antenna velocity. It then computes the error between the actual and desired antenna position and outputs the maximum control signal, assuming that the initial absolute angular error exceeds 0.8 degrees. This cycle of sampling and outputting the maximum command signal continues until the displacement error becomes less than 0.8 degrees. Then the sign of the command signal is determined from the rules displayed on the switching graph (Fig. 7) and the amplitude is taken as the product of the displacement error and the velocity.

As the displacement error approaches zero, the value of the velocity-error product becomes insignificant resulting in no appreciable control signal to eliminate the remaining finite error. To overcome this problem, a second limit is set at 0.15 degrees per second on the velocity axis. If the computer senses a velocity of less than this value as well as an absolute error of 0.8 degrees, then the error is multiplied by a factor of four to provide the output control signal.

4.3: Graphical Results From the Actual System Model

Graph #1 of position error versus time for a series of step input commands to the original system shows the present underdamped system response as simulated on the analogue computer. It appears to be quite nonlinear. Although torque limiters are in the system and these limits are reached for the inputs in question, the diode limiters used in the simulation provide rather soft voltage limits, so that the maximum velocity of the system is not well defined, but appears to be dependent on the input step size. It should be noted, however, that the overshoot

GRAPH # 2
Present System Model
Phase Plane Plot

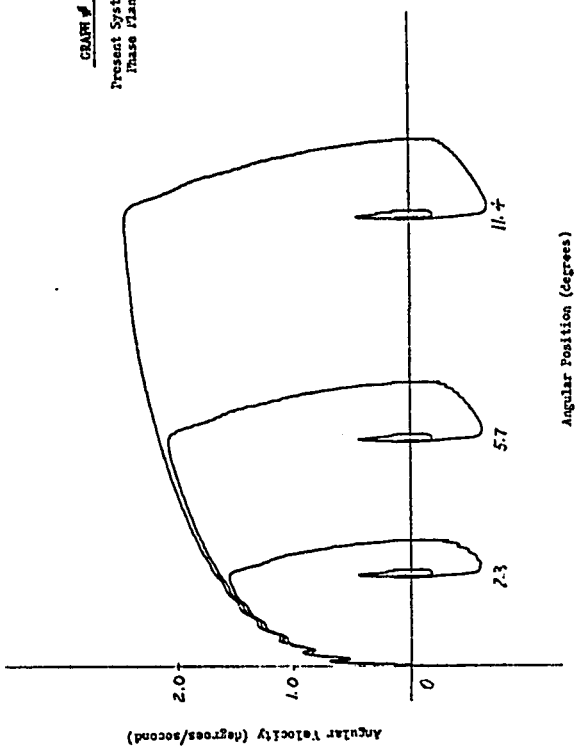

GRAPH # 4
Present System Model
Feedback Control Signal

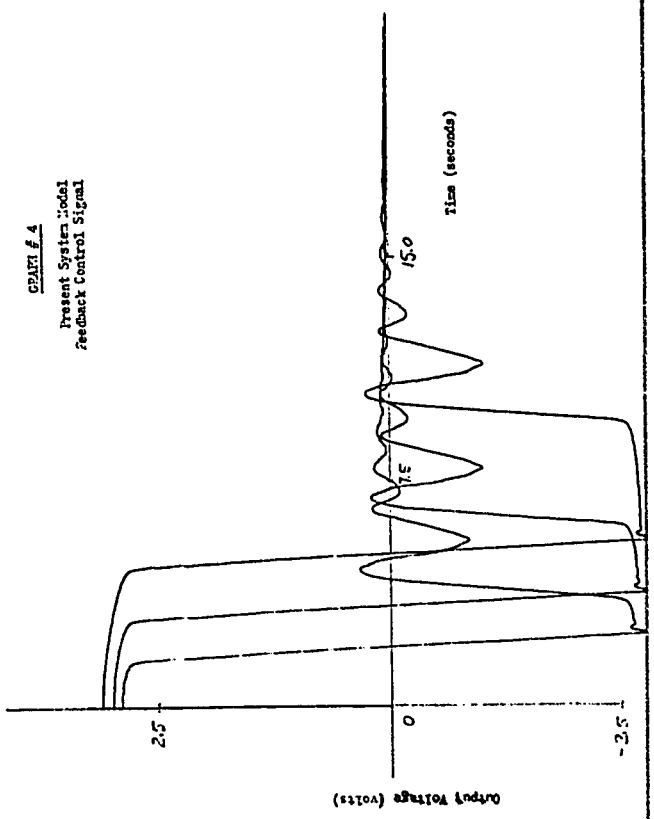

GRAPH # 1
Present System Model - Step Inputs
Position Error versus Time

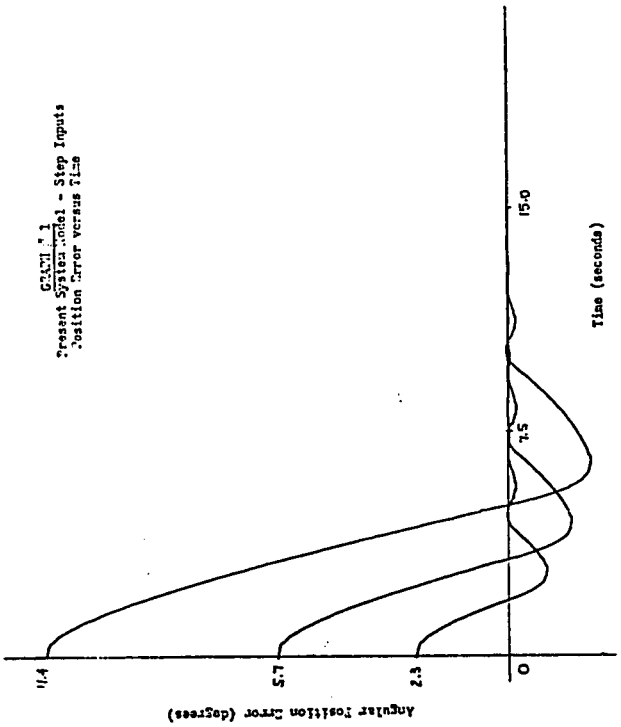

GRAPH # 3
Present System Model
Velocity Profile

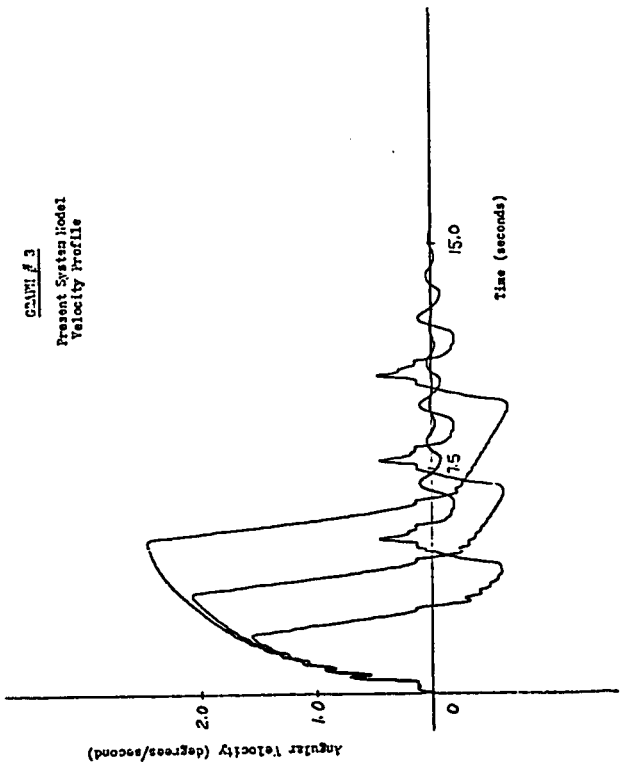

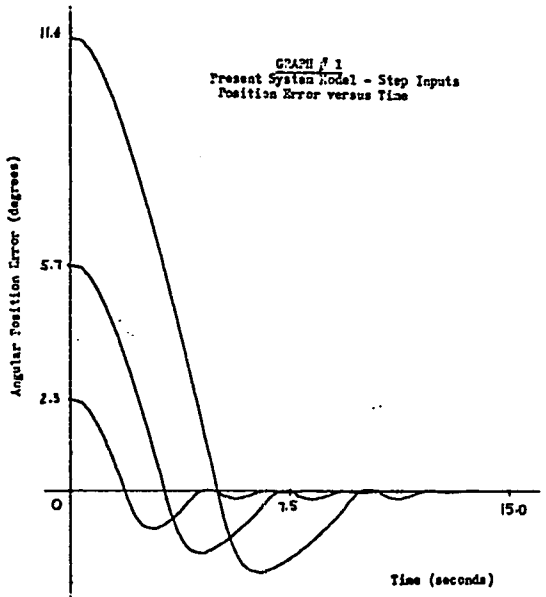

GRAPH # 1
Present System Model - Step Inputs
Position Error versus Time

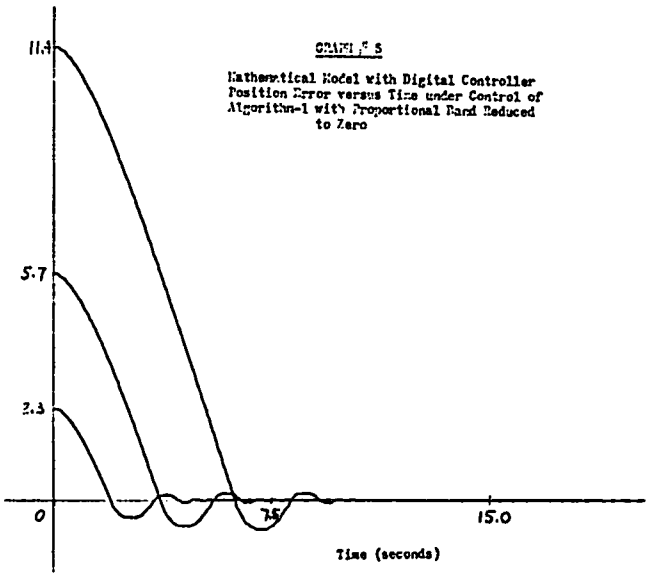

GRAPH # 5
Mathematical Model with Digital Controller
Position Error versus Time under Control of
Algorithm-1 with Proportional Band Reduced
to Zero

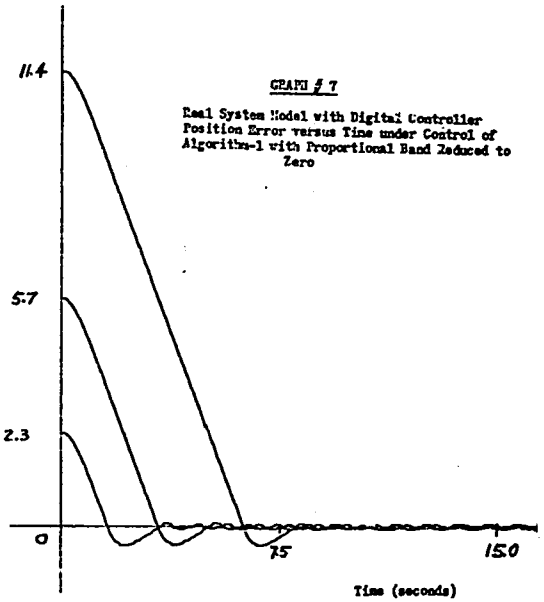

GRAPH # 7
Real System Model with Digital Controller
Position Error versus Time under Control of
Algorithm-1 with Proportional Band Reduced to
Zero

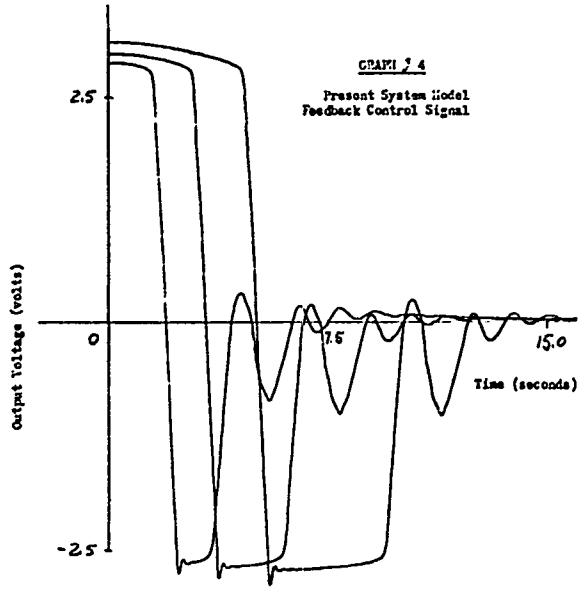

GRAPH # 4
Present System Model
Feedback Control Signal

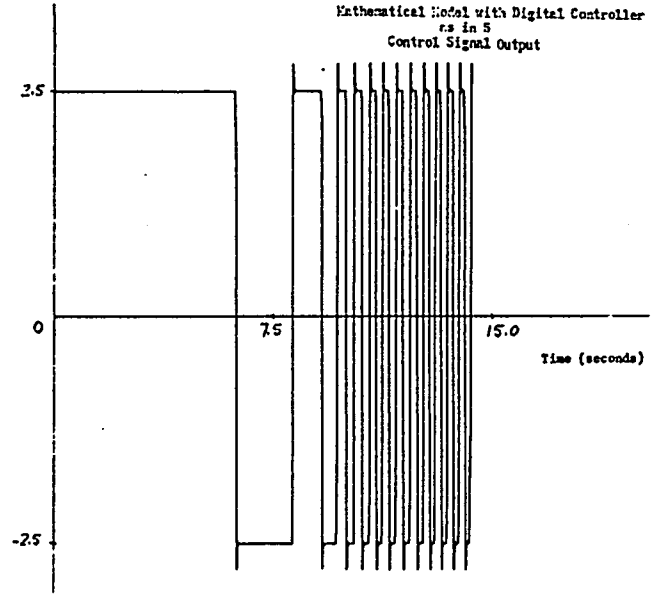

GRAPH # 6
Mathematical Model with Digital Controller
as in 5
Control Signal Output

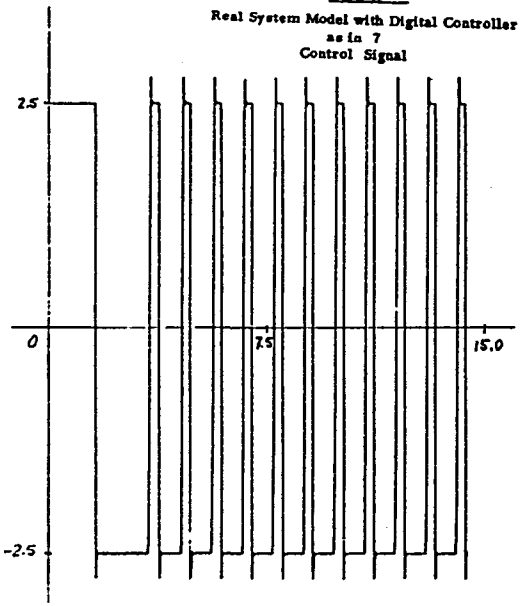

GRAPH #8
Real System Model with Digital Controller
as in 7
Control Signal

of the antenna is quite large and that a considerable improvement in performance could be achieved by elimination or reduction of that overshoot.

The phase plane plot of the system as shown in Graph #2 exhibits the sharp breaks which are characteristic of nonlinear behaviour. Graphs #3 and #4 respectively show the velocity profile and the corresponding control signals. These again emphasize the fact that we are dealing with a nonlinear system. The imprecise limiting of the control signal can clearly be seen. The velocity profile shows that the system velocity never reaches true saturation. This is also borne out by the position error plot which has no straight parts but rather presents a continuous curve.

4.4: Graphical Results from Algorithm-1

Graph #5 shows the error curve of the mathematical model for the standard step inputs under control of digital algorithm-1. In this instance the proportional or multiplicative band is reduced to zero. The resulting step response shows a considerably smaller overshoot and, as a result, a faster response time for any specific step input when compared with the realistic system and the present control scheme. However, using only a maximum control signal region for the system results in limit cycling which can be observed on graph #6. As can be seen from this control signal output corresponding to the error curve of the mathematical model the controller provides a bang-bang control. It can be noted here how much more precise the digital limiting of the control signal amplitude is when compared to the analogue limiting as shown in graph #4. Graph #6 demonstrates the complete symmetry of the model and its control as the antenna hunts around its desired position. With regard to graphs #5 and #6, if one considers the command input to be from the initial step input to the point of maximum overshoot

when the antenna is momentarily at rest, then one has an optimistic estimate of the true optimal control for that specific size of step input. If all the state variables of the system except for the position were zero at that instant then the true optimal control would indeed have been achieved for that particular step size. Any additional time required to dissipate any residual energy stored in the system and so reduce the remaining state variables to zero would necessarily increase the optimistic estimate. This estimate as measured from graph #5 is 0.6 seconds for the antenna to reach its final position from a point 0.8 degrees from that position.

It can be further seen from the three step responses shown on this graph that once the system reaches its saturating velocity, the time required to bring the antenna to rest is independent of the step size and remains constant.

Graph #7 shows the position error of the real system under control of algorithm-1. Comparing graph #7 with graph #5, where the latter is the position error of the mathematical model, one can readily see the similarity between the model and the actual system.

Graph #8 shows the control signal for the real system with algorithm-1. It indicates the same sort of limit cycle taking place as for the mathematical model (graph #6), but due to the counter torque in the system the positive and negative control signals are no longer of equal duration. This lack of symmetry in the limit cycle is a necessary part of the realistic control system due to the small constant torque on the antenna. This weight was added to ensure that in the case of a catastrophic power failure or similar mishap the antenna would not crash into its support stops but

GRAPH # 9

Real System Model with Digital Controller
Control Signal for Algorithm-1 with
Proportional Band of 1.6 Degrees

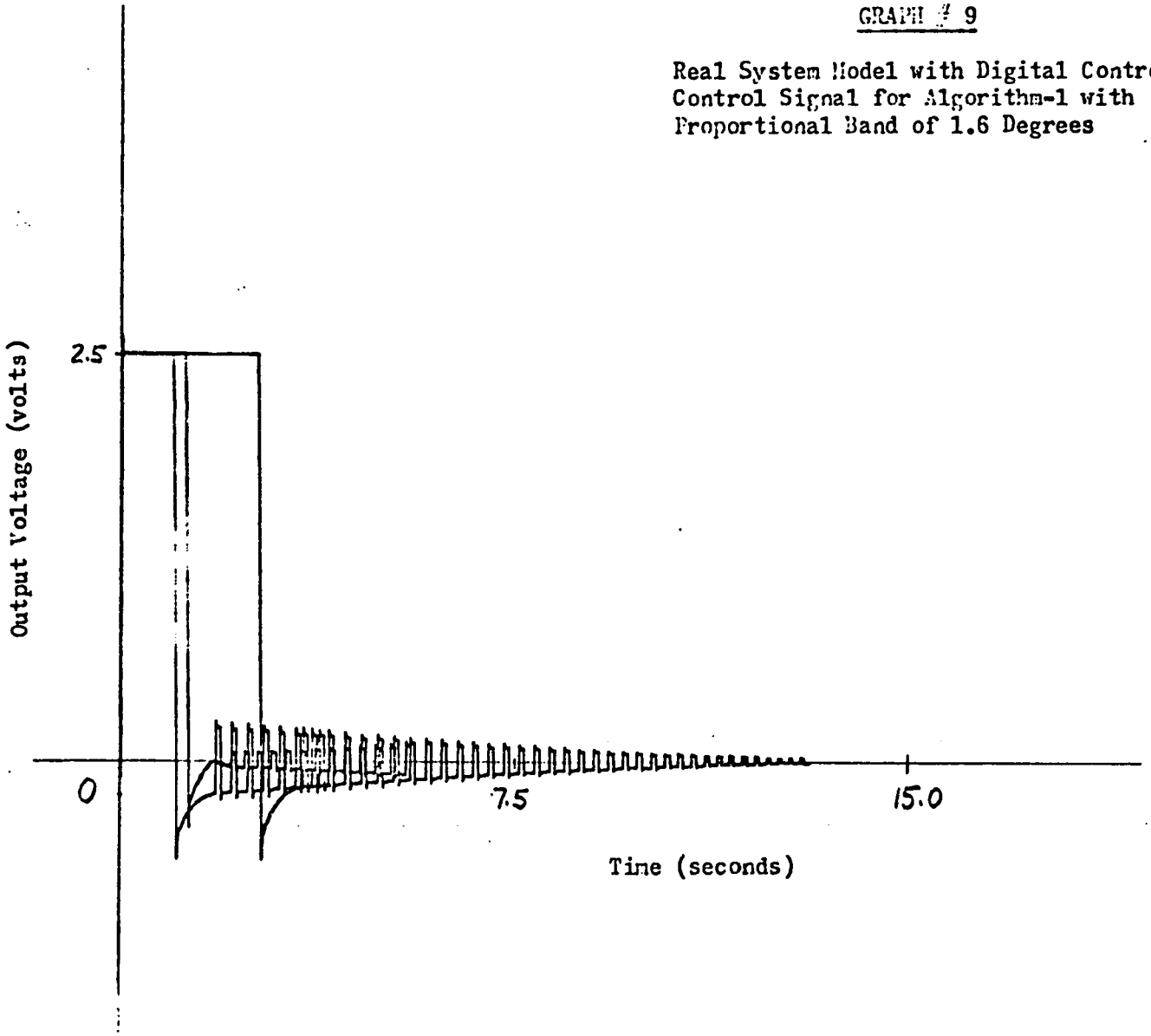

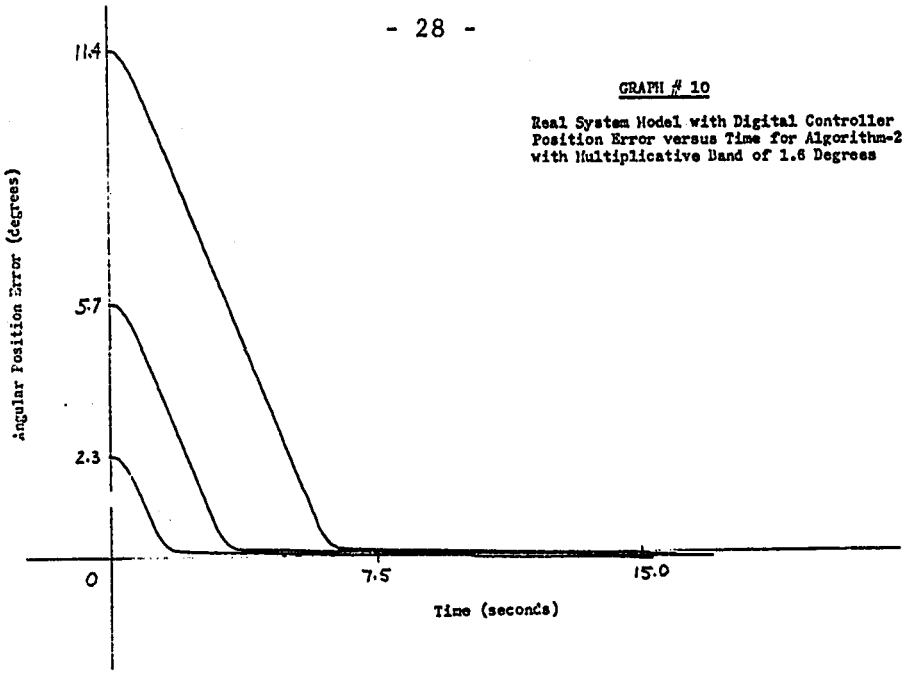

GRAPH # 10

Real System Model with Digital Controller
Position Error versus Time for Algorithm-2
with Multiplicative Band of 1.6 Degrees

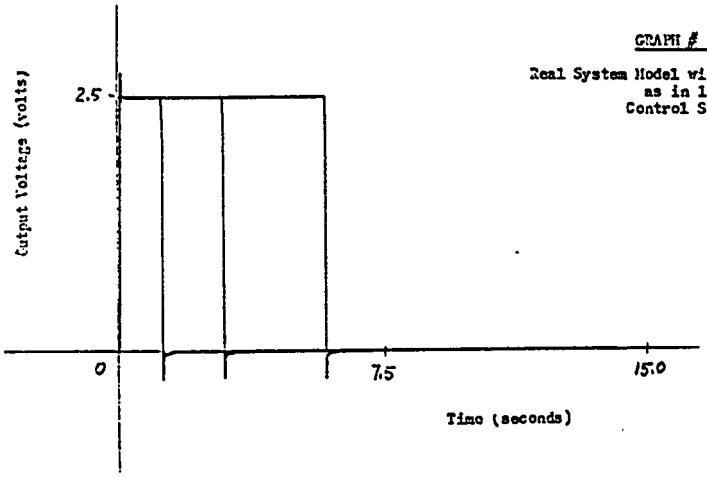

GRAPH # 11

Real System Model with Digital Controller
as in 10
Control Signal

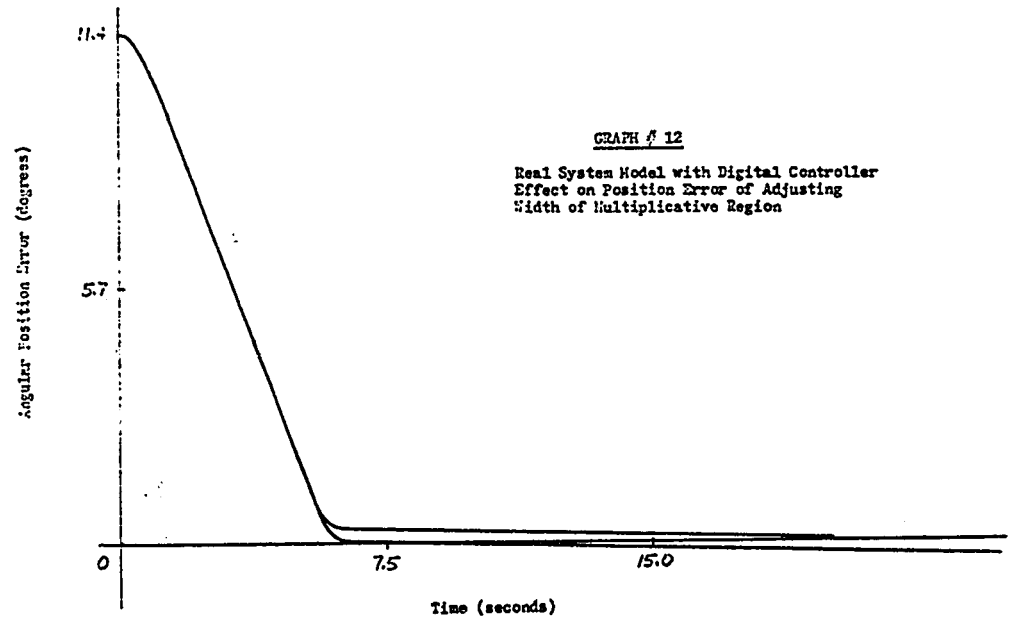

GRAPH # 12

Real System Model with Digital Controller
Effect on Position Error of Adjusting
Width of Multiplicative Region

rather turn to point upwards. The overshoot found on this and other control signal graphs is due to the plotter response alone and does not represent an overshoot of the D/A converter outputs.

Graph #9 shows the effect on the control signal of the introduction of the proportional region of 0.8 degrees into the algorithm. Here it can be seen that for certain values of the displacement error the system starts to become unstable as is demonstrated by the increasing control signal amplitude.

4.5: Graphical Results from Algorithm-2

Graph #10 shows the variable position error for the system under control of algorithm-2, which includes a 0.8 degree multiplicative control band. It should be noted that the system response for the entire range of step inputs no longer exhibits any overshoot so that its performance has been improved in this sense as compared with the initial system. The sensitivity of the controller for errors of 0.5 degrees or less is very poor, however, since the antenna will continue to drift through the zero error position while the output of the controller remains at zero. The corresponding control signal is shown in graph #11.

Although the control scheme is not very sensitive for small angular errors, it is very stable. An attempt to increase the sensitivity of the controller by making the control signal amplitude directly proportional to the error displacement would have meant reverting to the type of control provided by algorithm-1.

Graph #12 shows the effect that a variation in the width of the multiplicative region has on the antenna response. By increasing the

GRAPH # 13

Real System Model with Digital Controller
Phase Plane Plot for Algorithm-2

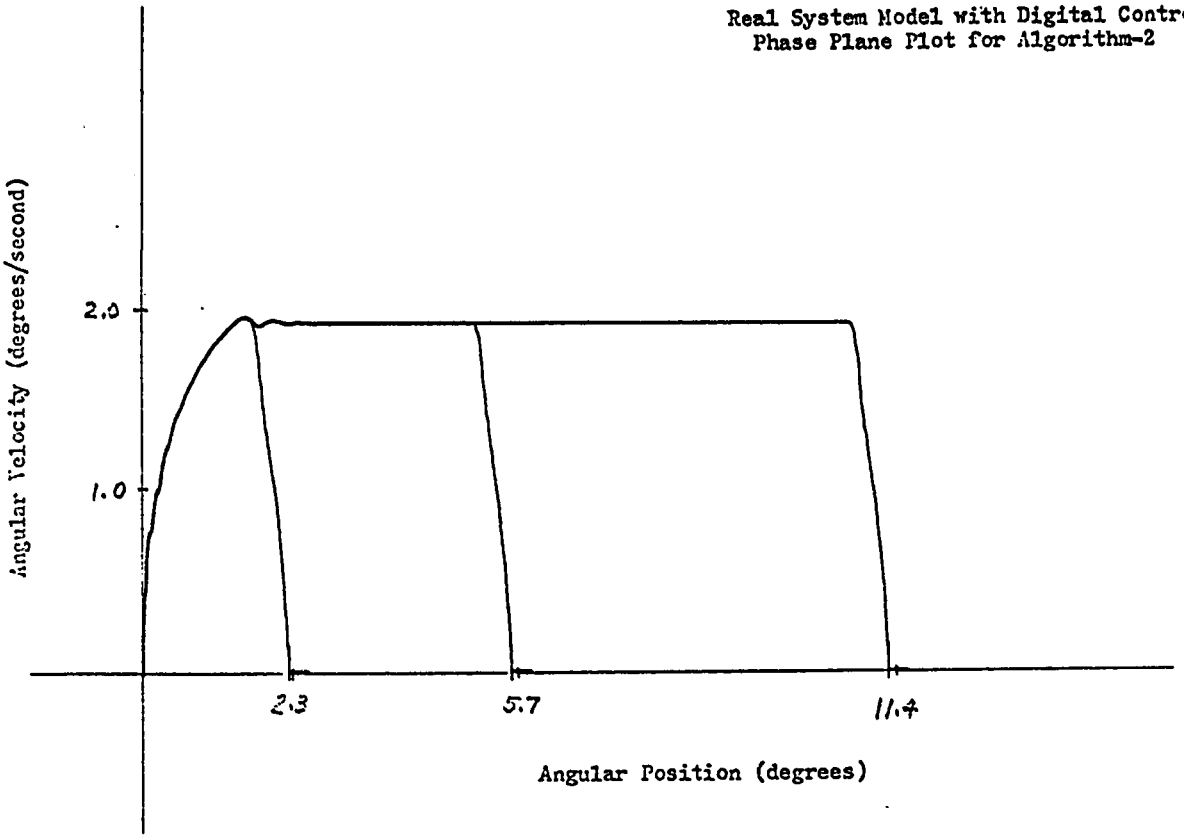

GRAPH # 14

Real System Model with Digital Controller
Velocity Profile for Algorithm-2

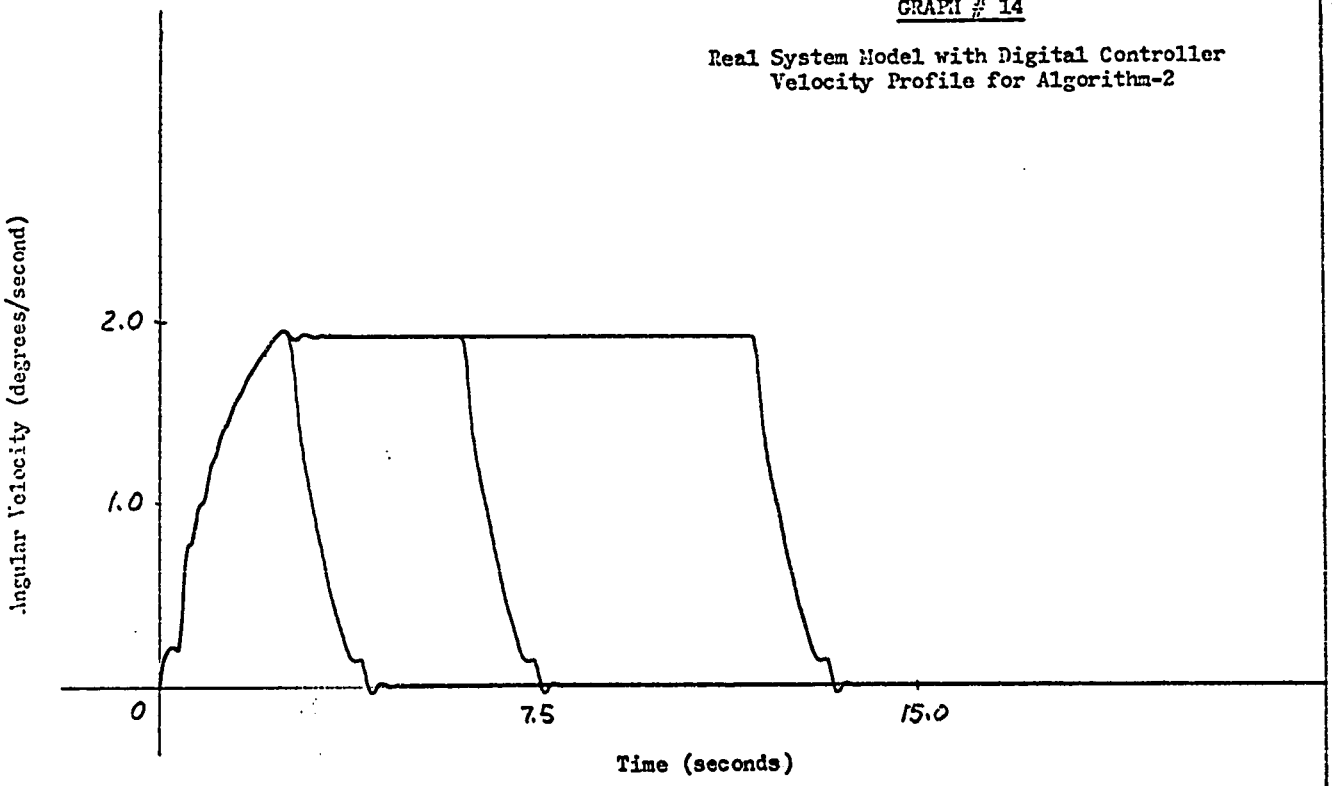

GRAPH # 1

Present System Model - Step Inputs
Position Error versus Time

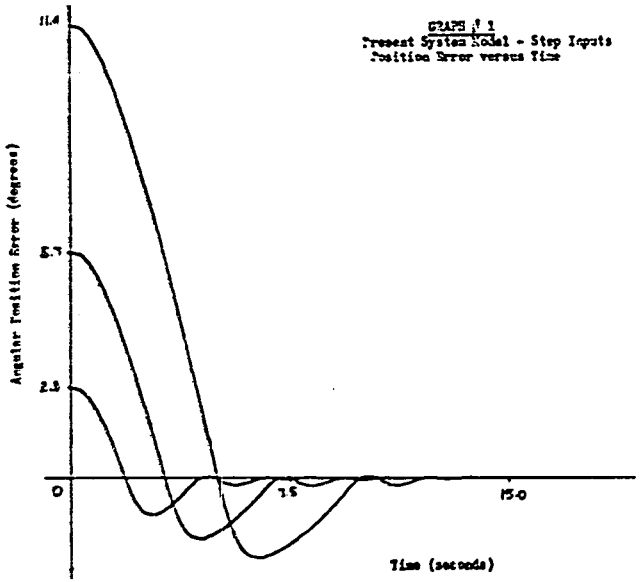

GRAPH # 15

Real System Model with Digital Controller
Position Error versus Time for Algorithm-3

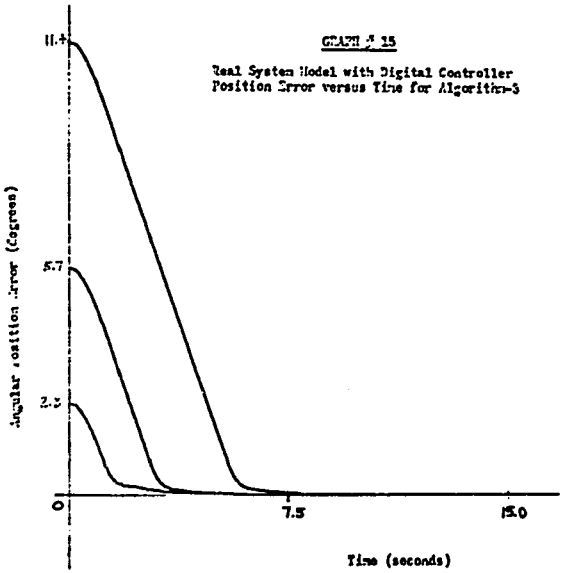

GRAPH # 16

Real System Model with Digital Controller
Phase Plane Plot for Algorithm-3

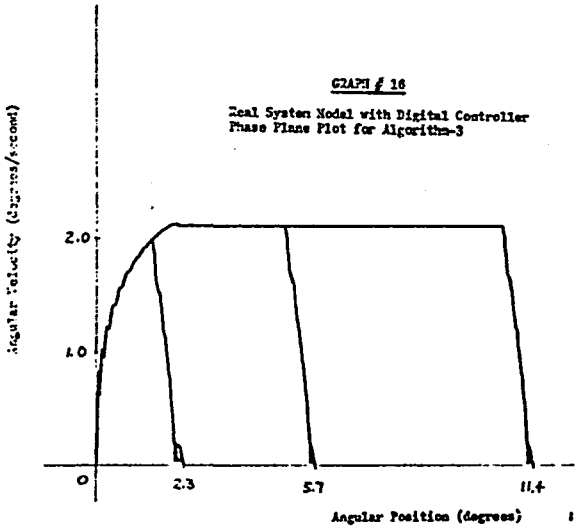

GRAPH # 4

Present System Model
Feedback Control Signal

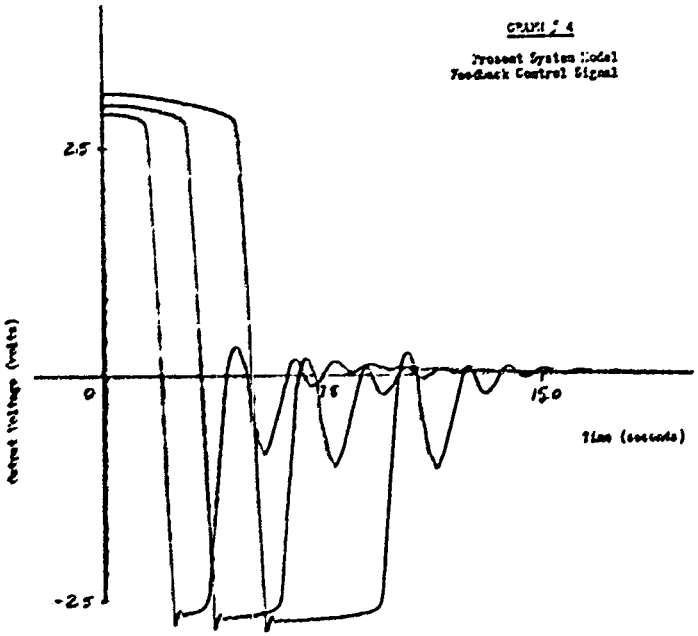

GRAPH # 18

Real System Model with Digital Controller
Control Signal for Algorithm-3

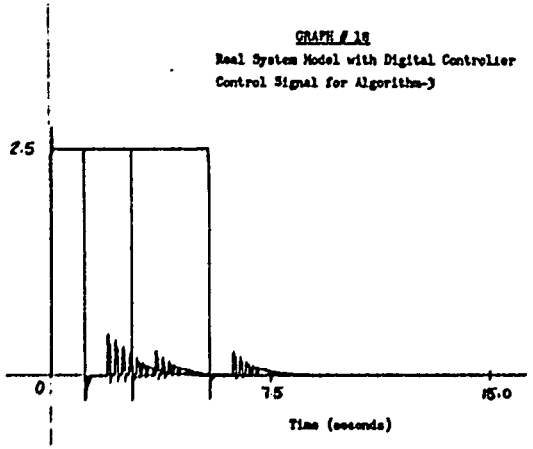

GRAPH # 17

Real System Model with Digital Controller
Velocity Profile for Algorithm-3

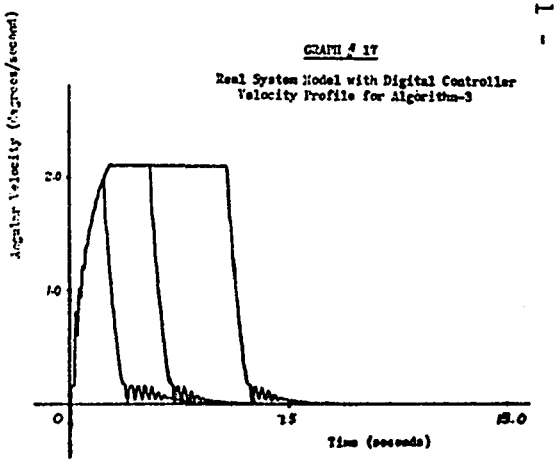

width of the region to 1.1 degrees the antenna is slowed earlier for the same step size. It then drifts slowly through the desired position as only the counter torque is acting on the system for small angular displacements. Similarly by reducing the region width to 0.5 degrees the braking action occurs at a later time. Graph #13 is the phase plane plot of algorithm-2. It bears a marked resemblance to the antenna velocity versus time plot (graph #14). From the velocity graph an indication of the effectiveness of different control schemes can be obtained. Thus it can simplify the choice of the minimum time controller. From the initial sampling instant until the region of multiplicative control is reached approximately 0.8 degrees from the final position, the antenna system is driven with the maximum available force. During this part the velocity graph is flat after an initial rise from zero. Then by the steepness of the final drop in velocity to zero, one can judge approximately which scheme is the most effective. Graphs #3, #14 and #17 each represent the antenna velocity.

4.6: Graphical Results from Algorithm-3

The four graphs numbered 15 through 18 show the system response under control of the final algorithm. This program includes two switching points, since only in this manner could the small error sensitivity of the system be improved without creating an unstable control. The first switching point at 0.8 degrees remains unaltered as does the type of multiplicative control until the antenna velocity becomes 0.15 degrees/second or less. Then the error control signal becomes proportional. In this case a multiple of four of the actual sampled error is used to obtain the control signal. In this fashion excellent small angle response is achieved as well as a good

response to large angular errors. The time taken for the system to reach its final position from a point 0.8 degrees away and at maximum velocity is approximately 1.2 seconds as measured from graph #15. The true optimal controller could conceivably reduce the settling time by as much as one-half or 0.6 seconds. Weighing the simplicity of the developed algorithm against the complexity of a program that might result in a true optimal response and taking into account the relative effectiveness of algorithm-3, it was considered that the latter provides a sufficiently close approximation of the true optimal control for step input responses to recommend it for implementation on the operational system. That algorithm-3 was indeed the best control program under evaluation can be seen by the steeper gradient of the velocity profile as the antenna nears its desired position. (See graphs #3, #14 and #17). An examination of the position error and control signal graphs provides further evidence.

The difference between the phase plot of graph #2 and graphs #13 and #16, where the latter represent the system under control of digital algorithms, can be attributed partly to the removal of the nonlinear limits on the summing amplifier and the removal of the compensation network. Under control of the algorithms the maximum velocity of the system is established more precisely due to the exact limiting of the control signal and the quick response of the controller. With the velocity constant for a considerable portion of the large step inputs and with no positional overshoot the phase plane plots of the latter two graphs have become simpler and reflect more closely the velocity-time graphs of the system.

4.7: Summary of the Experimental Results

The problem under consideration has been one of developing a simple but effective digital control scheme for a relatively complex control system which at present is operating in a non-optimal fashion with regard to its time response to step input commands.

To improve and possibly optimize the controller it was decided to approach the matter from the theoretical stand-point. An optimal control sequence was to be developed which could possibly be used on the actual system or one which could at least be used as the standard of performance for the actual system controller. It was also anticipated that the theoretical analysis of the system might yield a deeper understanding of the control process under consideration.

The development of a suitably linear model proved to be time consuming, but a model was developed which reflected the main characteristics of the real system response as far as a variety of step inputs was concerned. Then two methods were employed to attempt to arrive at an optimal theoretical solution for the simplified model.

First the state variable diagram corresponding to the theoretical model was derived and from it the A matrix as outlined in Appendix A. This A matrix could then be used as the input to a program developed by Dr. L. Birta and Mr. P. Trushel of NRC [4]. This algorithm was designed to obtain an open-loop optimal control sequence which would result in the minimum time solution for transferring the antenna to its desired position allowing for the bound on the control signal. Unfortunately, although the program has yielded accurate results for lower order systems, it has not provided any satisfactory minimum time solution in our case.

A second more straightforward method involving considerably more hand calculation was also applied to the problem. The technique is outlined by J. Tou [5]. This method involves the derivation of the state transition matrix from the A matrix. This derivation is described and carried out in Appendix B. For a fourth order system like ours this method involves the determination of a large number of Laplace transforms and their conversions to the time domain. The theory for this approach was outlined in Chapter III.

Again the theoretically obtained results, when compared with the actual system performance, proved to be quite unsatisfactory. This fact could be partially attributed to inaccuracies in the measurement of the system parameters or approximations made in the design of the model. Nevertheless this method appears to be very sensitive to variations in the values of the A matrix. These variations are transmitted and sometimes magnified in the process of deriving the transition matrix from the A matrix, and the process of iterative multiplication appears to accentuate the difference even more. As can be seen from graph #19, where both the theoretical and actual system response is plotted for a step input, the difference between the two curves is much larger than the difference in the time response between the actual system and the model as measured on the hybrid computer (graphs #5 and #7). This comparison is quite valid as in both the calculated and the measured system response the system is being driven with the control signal at its upper bound for the entire period of comparison.

As a result the digital control algorithm which yielded the best response was devised strictly on a basis of trial and error. The res-

ponse of the system to any particular algorithm could be readily evaluated on the hybrid computer, so that this method was both relatively quick and accurate. For this particular case the system had a velocity limit. As a result the velocity profile as well as the position error plot served as very useful indicators of the degree by which the control scheme fell short of a time optimal control. The superiority of one scheme over another was quickly determined by the comparison of the position error plots.

Several algorithms were evaluated which contained only one switch point between the region of maximum control and multiplicative or proportional control. None of these proved to result in a satisfactory response for both large and small angular step inputs. Only by introducing two switch points and a corresponding region of multiplicative as well as proportional control could a suitable time response and a pointing error of less than 0.2 degrees be achieved. M. Jafri's work [7] on multiplicative control proved to be of value for this program.

In the successful algorithm the type of control is dependent on both the angular error and the antenna velocity. For velocities less than 0.15 degrees per second the actual angular error is magnfied by a factor of four to yield the error signal. For velocities in excess of 0.15 degrees per second and displacement errors less than 0.8 degrees the control signal consists of the product of the absolute position error and the antenna velocity. This ability to vary the effective loop gain of the system by means of the digital controller for any desired range of error magnitudes greatly enhances our control capabilities. It provides us with the opportunity to shape the response of the system much more precisely and quickly than we could ever hope to achieve with normal compensation methods.

By increasing the gain of the system for most error magnitudes but decreasing the loop gain for the error region which causes system instability we greatly improve the system response for step inputs.

The results obtained from this program demonstrate a much tighter control of the antenna position with a considerably reduced response time of 7.3 seconds for an 11 degree step input, for instance, as compared with 13.0 seconds for the original system. Although this scheme is not truly optimal, it does approximate it very closely. The advantage of this control is its great stability in response to all possible step inputs. In an operational environment this characteristic is of utmost importance and although the system response takes approximately 8% longer than a true bang-bang controller for an 11 degree step input and as much as 40% longer for a 2.3 degree step, this time penalty seems to be unavoidable.

CONCLUSION

From the foregoing discussion it appears that for the design of optimal controllers for complicated, realistic, non-linear systems the quickest and surest method of determining an algorithm which yields near optimal results is by means of simulating such a system and any proposed control scheme either on a digital or hybrid computer. This seems to hold despite the sophisticated mathematical techniques available for optimization studies, which in no way guarantee any realistic solution for high order control systems.

Once a simulated model exists on the hybrid computer, one can determine the control scheme which yields the best results by experimentation with a variety of possible algorithms adapted to the control process in question. In our case the true optimal controller could be closely approximated by applying a bang-bang control scheme and measuring from the position error graph the time taken by the system to reach its final state. By this means a very reasonable time estimate of the optimal control could be obtained.

Thus a suitable and effective algorithm for the system was determined in a relatively short time when compared with the calculations required to obtain similar theoretical sequences. The effects of the algorithms could be observed in real-time and even "compressed real-time" and then could be altered and refined in order to be as effective as possible.

The control scheme which was eventually adopted meets the specifications of a short response time to a step input with a pointing error of less than ± 0.1 degrees. The controller ensures a stable operating system under all input conditions and the stress and wear on the system components is greatly reduced from the present.

The simplicity of the program from the point of view of additional hardware requirements and the amount of central processor time is another important design objective which has been met.

The maximum overshoot for the initial system step response of 11 degrees was approximately 2.5 degrees. With the digital controller this is reduced to zero. At the same time the time response for the same step input has been decreased from 13.0 seconds to 7.3 seconds with a pointing error of less than $\pm$0.1 degrees.

Besides being useful in the Designated Position Mode, the algorithm developed appears to be equally useable for the control of the antenna in the Steering Tape Mode.

APPENDIX "A"

To determine the A matrix we use the relationship

$$\frac{d\bar{x}(t)}{dt} = A\,\bar{x}(t) \qquad \text{(A-1)}$$

where $\bar{x} = \begin{bmatrix} x_1 \\ x_2 \\ x_3 \\ x_4 \end{bmatrix}$

Using the flow graph and substituting into equation (A-1) for $\bar{x}$, we get

$$\begin{bmatrix} \dot{x}_1 \\ \dot{x}_2 \\ \dot{x}_3 \\ \dot{x}_4 \end{bmatrix} = \begin{bmatrix} 0 & C & B & A \\ 0 & -D & 1 & 0 \\ 0 & -E & 0 & 1 \\ 0 & -F & 0 & 0 \end{bmatrix} \begin{bmatrix} x_1 \\ x_2 \\ x_3 \\ x_4 \end{bmatrix}$$

$$\therefore \; A = \begin{bmatrix} 0 & C & B & A \\ 0 & -D & 1 & 0 \\ 0 & -E & 0 & 1 \\ 0 & -F & 0 & 0 \end{bmatrix}$$

To determine the feedback matrix B, the following equations can be derived from Figure 5 by inspection:

$$x_1(T^+) = x_1(T)$$
$$x_2(T^+) = x_2(T)$$
$$x_3(T^+) = x_3(T)$$
$$x_4(T^+) = x_4(T)$$
$$m(T^+) = r(T) - x_1(T)$$
$$r(T^+) = r(T)$$

thus if $\bar{v} = \begin{bmatrix} r \\ \bar{x} \\ m \end{bmatrix} = \begin{bmatrix} r \\ x_1 \\ x_2 \\ x_3 \\ x_4 \end{bmatrix}$

then $\bar{v}(T^+) = B\,\bar{v}(T)$ can be used to determine B.

$$\therefore \quad \begin{bmatrix} r(T^+) \\ x_1(T^+) \\ x_2(T^+) \\ x_3(T^+) \\ x_4(T^+) \\ m(T^+) \end{bmatrix} = \begin{bmatrix} 1 & 0 & 0 & 0 & 0 & 0 \\ 0 & 1 & 0 & 0 & 0 & 0 \\ 0 & 0 & 1 & 0 & 0 & 0 \\ 0 & 0 & 0 & 1 & 0 & 0 \\ 0 & 0 & 0 & 0 & 1 & 0 \\ 1 & -1 & 0 & 0 & 0 & 0 \end{bmatrix} \begin{bmatrix} r(T) \\ x_1(T) \\ x_2(T) \\ x_3(T) \\ x_4(T) \\ m(T) \end{bmatrix}$$

where B is the above 6 x 6 matrix.

APPENDIX "B"

Determination of the Overall Transition Matrix $\underline{\Phi}(t)$.

$\underline{\Phi}(t)$ is the overall transition matrix including the process state variables as well as the input state variables. It is defined by the state differential equation:

$$\frac{d\bar{v}(t)}{dt} = \underline{\Phi}(t)\,\bar{v}(t)$$

One can determine $\phi(t)$, the transition matrix of the plant, either from the coefficient matrix A or the state variable diagram. We have selected the method of deriving $\phi(t)$ from A.

As $\phi(t)$ is also defined by the equality

$$\phi(t) \equiv e^{At}$$

we can find the desired matrix by determining the inverse Laplace transform of $[sI - A]$.

Now $$[sI - A] = \begin{bmatrix} s & -c & -b & -a \\ 0 & s+d & -1 & 0 \\ 0 & e & s & -1 \\ 0 & f & 0 & s \end{bmatrix}$$

and the determinant $\Delta = s(s^3 + ds^2 + es + f)$

From this we get

$$\phi(t) = \mathcal{L}^{-1}\left\{ \frac{1}{\Delta} \begin{bmatrix} s^3+ds^2+es+f & cs^2-(eb+af)s-fb & bs^2+cs+bd-af & as^2+(ae+b)s+c+af+eb \\ 0 & s^3 & s^2 & s \\ 0 & -s(es+f) & s^2(s+d) & s(s+d) \\ 0 & -fs^2 & fs & s^2(s+d)+es \end{bmatrix} \right\}$$

Thus we have for the first row:

$$\phi_{11}(t) = \mathcal{L}^{-1}\left\{ \frac{1}{s} \right\}$$

$$\phi_{12}(t) = \mathcal{L}^{-1}\left\{ \frac{cs^2-(eb+af)s-fb}{s(s^3+ds^2+es+f)} \right\}$$

$$\phi_{13}(t) = \mathcal{L}^{-1}\left\{ \frac{bs^2+cs+bd-af}{s(s^3+ds^2+es+f)} \right\}$$

$$\phi_{14}(t) = \mathcal{L}^{-1}\left\{ \frac{as^2+(ae+b)s+c+af+eb}{s(s^3+ds^2+es+f)} \right\}$$

Once all values of $\phi(t)$ have been calculated, the overall transition matrix $\underline{\Phi}(t)$ can be developed from the plant transition matrix by the theory outlined in Section 3.2, where $\underline{\Phi}(t)$ is defined as

$$\underline{\Phi}(t) = \begin{bmatrix} R(t) & 0 \\ h(t) & \phi(t) \end{bmatrix}$$

The components of $\Phi(T)$ were calculated to be

$$\Phi_{11}(T) = 1 \qquad \Phi_{12}(T) = \Phi_{13}(T) = \Phi_{14}(T) = \Phi_{15}(T) = \Phi_{16}(T) = 0$$

$$\Phi_{21}(T) = 0 \qquad \Phi_{22}(T) = 1$$

$$\Phi_{23}(T) = .125\left[3.42 - 7.45\,e^{-.104T} + 12.3\,e^{-1.71T} - 8.27\,e^{-2.57T}\right]$$

$$\Phi_{24}(T) = -.427\left[1.37 - .512\,e^{-.104T} - 1.47\,e^{-1.71T} + .606\,e^{-2.57T}\right]$$

$$\Phi_{25}(T) = .586\left[4.08 - 3.63\,e^{-.104T} - .627\,e^{-1.71T} + .175\,e^{-2.57T}\right]$$

$$\Phi_{26}(T) = .586\left[\frac{3.66 + 1.86T}{.456} - 43.2 + 34.9\,e^{-.104T} + .367\,e^{-1.71T} - .068\,e^{-2.57T}\right]$$

$$\Phi_{31}(T) = \Phi_{32}(T) = 0$$

$$\Phi_{33}(T) = .0027\,e^{-.104T} + 3.11\,e^{-2.57T} - 2.20\,e^{-1.71T}$$

$$\Phi_{34}(T) = -.0263\,e^{-.104T} + 1.24\,e^{-1.71T} - 1.21\,e^{-2.57T}$$

$$\Phi_{35}(T) = .252\,e^{-.104T} - .725\,e^{-1.71T} + .471\,e^{-2.57T}$$

$$\Phi_{36}(T) = 2.20 - 2.43\,e^{-.104T} + .424\,e^{-1.71T} - .183\,e^{-2.57T}$$

$$\Phi_{41}(T) = \Phi_{42}(T) = 0$$

$$\Phi_{43}(T) = 4.83\left[.003\,e^{-.104T} - 1.17\,e^{-1.71T} + 1.17\,e^{-2.57T}\right]$$

$$\Phi_{44}(T) = -.112\,e^{-.104T} + 3.31\,e^{-1.71T} - 2.21\,e^{-2.57T}$$

$$\Phi_{45}(T) = 1.08\,e^{-.104T} - 1.94\,e^{-1.71T} + .854\,e^{-2.57T}$$

$$\Phi_{46}(T) = 9.61 - 10.4\,e^{-.104T} + 1.14\,e^{-1.71T} - .335\,e^{-2.57T}$$

$$\Phi_{51}(T) = \Phi_{52}(T) = 0$$

$$\Phi_{53}(T) = .456\left[.026\,e^{-.104T} - 1.24\,e^{-1.71T} + 1.21\,e^{-2.57T}\right]$$

$$\Phi_{54}(T) = .456\left[.252\,e^{-.104T} - .725\,e^{-1.71T} + .471\,e^{-2.57T}\right]$$

$$\Phi_{55}(T) = 1.11\,e^{-.104T} - .193\,e^{-1.71T} + .083\,e^{-2.57T}$$

$$\Phi_{56}(T) = 10.6 - 10.7\,e^{-.104T} + .113\,e^{-1.71T} - .032\,e^{-2.57T}$$

$$\Phi_{61}(T) = \Phi_{62}(T) = \Phi_{63}(T) = \Phi_{64}(T) = \Phi_{65}(T) = 0$$

$$\Phi_{66}(T) = 1$$

APPENDIX C

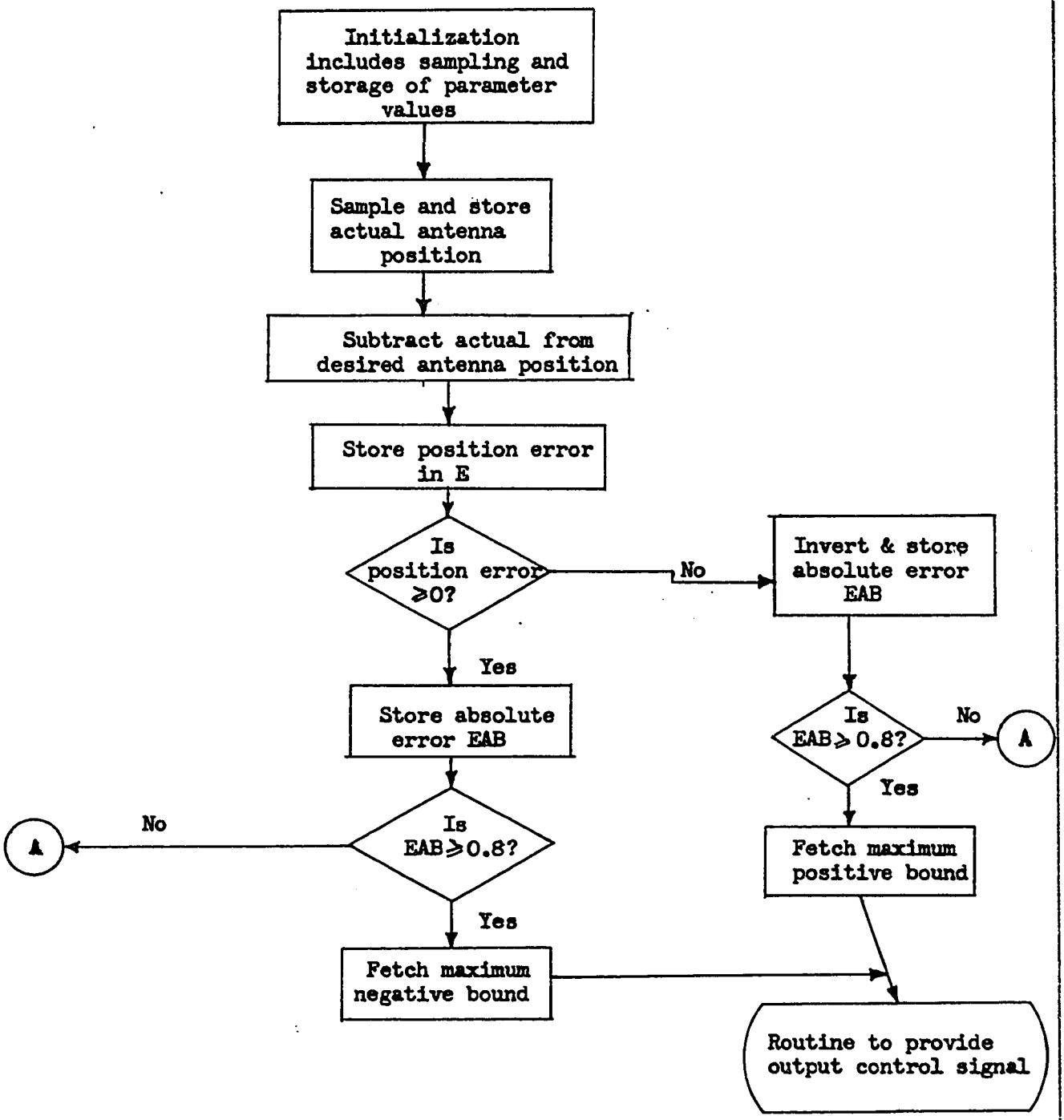
Initialization includes sampling and storage of parameter values
Sample and store actual antenna position
Subtract actual from desired antenna position
Store position error in E
Is position error ≥0?
No
Invert & store absolute error EAB
Yes
Store absolute error EAB
Is EAB≥0.8?
No
A
Yes
Fetch maximum positive bound
Is EAB≥0.8?
No
A
Yes
Fetch maximum negative bound
Routine to provide output control signal

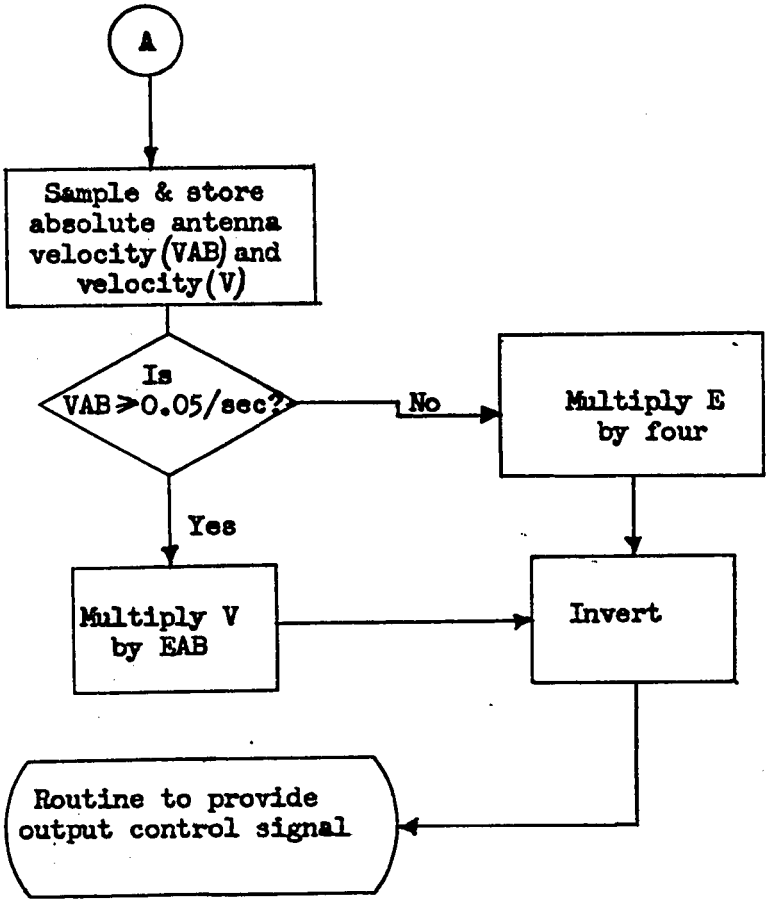
A
Sample & store absolute antenna velocity (VAB) and velocity (V)
Is VAB ≥ 0.05/sec?
No
Multiply E by four
Yes
Multiply V by EAB
Invert
Routine to provide output control signal

REFERENCES

1 Sanders, W.H. et al "The Acquisition and Tracking Control System for Canada's First Satellite Communications Station", DCF Systems Limited Report, pg.18, 1966.

2 Heikinen, R.R. "Analog Computer Study of Control and Drive System for 85 Ft AZ-EL Antenna", Dalmo Victor Company Report R-3020-3686, 1964.

3 Dolan, J.A. and Findeis, J.H. "Hybrid Simulation of the Mill Village Ground Station Antenna Control System", Department of Transport Report CRD-RE-146-1, May 1966.

4 Birta, L.G. and Trushel, P.J. "A Comparative Study of Four Implementations of a Dynamic Optimization Scheme", National Research Council Report AC-86, pp. 1-11, May 29, 1968.

5 Tou, J.T. "Modern Control Theory", McGraw Hill, New York, pp. 130-152, 1964.

6 Bellman, R., I. Glicksberg and O. Gross "On the Bang-Bang Control Problem", Quarterly Applied Mathematics, vol. 14, pp. 11-18, 1956.

7 Jafri, M.N. "Study of Certain Aspects of a Class of Nonlinear Multiplicative Systems", Doctoral dissertation, University of Ottawa, June 1967.

BIBLIOGRAPHY

Athans, M. and Falb, P.L. "Optimal Control", McGraw Hill, New York, 1966.

Brown, K.R. and Johnson, G.W. "Real-time Optimal Guidance", IEEE Transactions on Automatic Control, pg. 501, October 1967.

Douglass, J.W. "Optimum Seeking Methods", Prentice-Hall, New York, 1964.

Gibson, J.E. "A Set of Standard Specifications For Linear Automatic Control Systems", AIEE Transactions, Part II, Vol. 80, pp. 65-77, May 1961.

Giese, C. "State Variable Difference Methods for Digital Simulation", Simulation, Vol. 8, pp. 263-271, May 1967.

Kingma, Y.J. "Analog Simulators for Digital Controllers", Simulation, Vol. 10, pp. 65-68, February 1968.

Knowles, J.B. and Edwards, R. "Aspects of Subrate Digital Control Systems", Proceedings of IEE, Vol. 113, No. 11, pp. 1893-1901, November 1966.

Kohr, R.H. "On the Identification of Linear and Nonlinear Systems", Simulation, Vol. 8, pp. 165-174, March 1967.

Kuo, B.C. "Automatic Control Systems", Prentice-Hall, Englewood Cliffs, N.J., 1967.

Lee, Y.S. "A Time-Optimal Adaptive Control System in Adaptive Switching Hypersurface", IEEE Transactions on Electronic Computers, pg. 367, August 1967.

Merriam, C.W. "Optimization Theory and Design of Feedback Control Systems", McGraw Hill, New York, 1964.

Mugele, R.A. "A Nonlinear Digital Optimization Program for Process Control Systems", SJCC Proceedings, Vol. 21, pp. 15-32, 1962.

Thaler, G.J. and Brown, R.G. "Analysis and Design of Feedback Control Systems", McGraw Hill, New York, pp. 433-477, 1960.

BIOGRAPHICAL DATA

John Herbert Findeis was born on March 17, 1940. He studied for four years at the Royal Military College, Kingston, and received his Bachelor of Engineering degree from there in 1962. After spending three years in the RCAF, he joined the Department of Transport in 1965. Working for the Department on the Mill Village Project, provided him with the basic material for his thesis. He recently joined the Royal Canadian Mounted Police as a computer systems engineer.